Biological Journal of the Linnean Society, 2019, **128**, 700–724. With 9 figures.

Ontogeny and evolution of the sound-generating structures in the infraorder Delphinida (Odontoceti: Delphinida)

GUILHERME FRAINER[1,2,3,*], IGNACIO B. MORENO[1,2], NATHALIA SERPA[1,2], ANDERS GALATIUS[4], DIRK WIEDERMANN[5] and STEFAN HUGGENBERGER[3]

[1]*Programa de Pós-Graduação em Biologia Animal, Departamento de Zoologia, Universidade Federal do Rio Grande do Sul, 91540-000, Porto Alegre, Brazil*
[2]*Centro de Estudos Costeiros, Limnológicos e Marinhos (CECLIMAR/UFRGS), Campus Litoral Norte, Universidade Federal do Rio Grande do Sul, 95625-000, Imbé, Brazil*
[3]*Department II of Anatomy, University of Cologne, 50924, Cologne, Germany*
[4]*Department of Bioscience, Aarhus University, 4000 Roskilde, Denmark*
[5]*Max Planck Institute for Metabolism Research, 50931, Cologne, Germany*

Received 5 June 2019; revised 5 July 2019; accepted for publication 5 July 2019

The ontogeny of the structures involved in sound generation and modulation in dolphins was investigated through a comparison of the soft nasal structures of foetal, perinatal, neonatal and adult specimens of Pontoporiidae, Phocoenidae and Delphinidae. Foetal samples were sectioned at 10 µm in the saggital and coronal planes, and stained for histological examination. Computed tomography and magentic resonance imaging scan series were combined with new data to represent the ontogenetic stages of the three groups. The images were analysed in 3D-Slicer to characterize the general head topography. The origins of the melon and the vestibular air sac were detected between Carnegie stages C16 and F22. The three groups analysed showed distinct formation of the nasal plug and nasal plug muscles, mainly with regard to the loss of fat pathways (or their maintenance in Pontoporiidae) and the development of the nasal plug muscles on both sides (during perinatal development of Phocoenidae) or just on the left side (during postnatal development in Delphinidae). Broadband vocalizing delphinidans might have evolved under heterochronic events acting on the formation of sound-generating structures such as the rostrum and vestibular air sacs, and on the transformation of the branches of the melon, probably leading to a reduced directionality of the sonar beam.

ADDITIONAL KEYWORDS: character transformation – directionality – echolocation – evolutionary theory – heterochrony – systematics – toothed whales.

INTRODUCTION

A substantial part of the shape variation among biological organisms is due to changes in ontogenetic processes (Gould, 1977; Alberch *et al.*, 1979) promoted by variations in the regulation of gene expression domains during development (Laland *et al.*, 2015). According to Huxley (1942), the modern evolutionary synthesis combines Mendelian inheritance with Darwin's (1859) prerogative for natural selection, although the shape (i.e. character) transformation remained unexplained until recent advances in the field of evolutionary developmental biology (West-Eberhard, 2003). However, only a few studies have integrated this topic into systematics (Fink, 1982; De Queiroz, 1985; Kluge, 1985; de Pinna, 1991). Kluge (1985) pointed out that observations on ontogeny could support homology determinations and also polarize the character transformation by defining the direction of such changes (De Queiroz, 1985; Kluge, 1985). Although cetaceans may represent didactic organisms with regard to interpreting evolutionary theory (Thewissen *et al.*, 2006; Moran *et al.*, 2011), the evolution of specialized soft tissue organs for the generation of the sonar beam for echolocation in

*Corresponding author. E-mail: gui.frainer@gmail.com

odontocetes remains largely unknown (Morisaka & Connor, 2007; Galatius *et al.*, 2018).

Odontocetes have evolved a complex echolocation-based system for navigation and hunting which allowed them to explore deep, pelagic, shallow and freshwater environments (Au, 2000). Lindberg & Pyenson (2007) proposed that the origin of echolocation in this group dates from the early Oligocene (33.9–28.4 Mya) and is related to nocturnal epipelagic feeding on cephalopods and demersal fishes that perform diel migration from deep to surface waters at night. The authors (Lindberg & Pyenson, 2007) pointed out that morphological innovations related to the advent of echolocation in fossils were apparent in, for example, the transition from heterodont to homodont forms, the origin of an asymmetric skull (Heyning, 1989; Cranford *et al.*, 1996), and the enlargement of the brain (Marino *et al.*, 2004; Huggenberger, 2008; Oelschläger *et al.*, 2010). Recent studies have proposed that echolocation arose about 32 Mya as evidenced by decreasing body size and cochlear length in some stem odontocetes that were presumably capable of perceiving ultrasonic sounds (Geisler *et al.*, 2014; Churchill *et al.*, 2016). Additionally, even more specialized echolocating odontocetes from 18 Mya appear to have evolved an inner ear morphology to allow perception of narrow-band high frequency (NHBF) sounds (Galatius *et al.*, 2018). However, it seems that not only was the echolocation system responsible for enlargement of the brain in odontocetes but so too were social challenges, as evidenced by the richness of their social repertoire, particularly in delphinids (Huggenberger, 2008; Fox *et al.*, 2017). Here, acoustic communication was probably a very important function to establish complex social societies in the aquatic environment (Au, 2000).

Echolocation (i.e. clicks) and social (e.g. burst-clicks and whistles) sounds are both produced and modulated in the epicranial (nasal) complex of dolphins, respectively to the right and left (Madsen *et al.*, 2013) MLDB (monkey/phonic-lips dorsal bursae) complexes. These lip-like valves of the nasal passage (phonic lips, or Valva nasalis intermedia) and small fat bodies (posterior, Corpus adiposum nasalis posterior; anterior, Corpus adiposum nasalis anterior, dorsal bursae) are positioned on both sides of the nasal passage, a few centimetres below the blowhole in dolphins and porpoises (Cranford *et al.*, 1996). The initial sound waves of both vocalizations interact with the skull, a dense connective tissue theca and an air sac system surrounding the acoustic apparatus (Wei *et al.*, 2017). The sound is collimated forward through first the tissue of or near the nasal plugs (Valva nasalis ventralis), i.e. paired masses of connective tissue interspersed with muscle fibres just anterior to each nasal passage (Harper *et al.*, 2008), and then the melon (Corpus adiposum nasalis terminalis) into the environment (Wei *et al.*, 2017).

In this study, the comparative anatomy of the soft nasal tissues from foetuses to adults of three related odontocete groups were investigated (1) to identify morphology-based ontogenetic transformations; and, from a cladistic point of view, (2) to determine the heterochronic processes involved in major adaptations for sound production in these echolocating marine mammals. Although toothed whale evolution has been inextricably related to the ability to echolocate, a few studies have addressed the biosonar anatomy – and its development – in the light of phylogenetics and evolution (Kleinenberg & Yablokov, 1958; Mead, 1975; Heyning, 1989; McKenna *et al.*, 2012).

MATERIAL AND METHODS

Development of the main soft nasal structures involved in sound generation was investigated by comparing foetal, perinatal, neonatal and adult specimens of three odontocete families (Pontoporiidae, Phocoenidae and Delphinidae), as indicated in Table 1. Foetuses were classified according to the Carnegie/Foetal stages proposed by Thewissen & Heyning (2007). In this study, different morphological techniques were used to investigate the nasal tissue transformation throughout ontogeny as described below.

Microscopic analysis

All foetuses were fixed in 10% formalin, dehydrated and embedded in paraffin for processing. The samples were sectioned at 10 µm in the saggital or coronal plane, and stained with azan, and haematoxylin and eosin (H&E). Except for the sections of *Delphinus* (TBS 199) and *Pontoporia* (MM 35), all sections were housed in the extended cetacean embryological collection located at the Dr. Senckenbergische Anatomie (SAI) of the Johann Wolfgang Goethe Universität in Frankfurt am Main, Germany. The sections were scanned at 3200 dpi using an EPSON L220 digital scanner, then edited and aligned in Adobe Photoshop. The image series were converted to DICOM format using the DICOM import and export plugin for ImageJ (https://imagej.nih.gov/ij/) and analysed in 3D-Slicer (http://slicer.org/) to characterize and demonstrate the topographical arrangement of the early tissues surrounding the nasal cartilage (for 3D reconstruction, see below). Additional information regarding the morphogenesis of the narwhal (*Monodon monoceros*) head were taken from Comtesse-Weidner (2007).

Table 1. Details of the specimens examined in this study

Species	Code	Structure	Stage	Size* (mm)	Fixation	Method applied
Family Platanistidae						
Platanista gangetica	SAI no number	Head	Adult	?	?	CT†
Family Ziphiidae						
Mesoplodon sp.	SAI no number	Head	Adult	?	?	CT
Family Iniidae						
Inia geoffrensis	SAI no number	Head	Adult	?	?	CT†
Family Pontoporiidae						
Pontoporia blainvillei	GEMARS 1465	Head	Adult	1381	Frozen	CT/MRI/DS
Pontoporia blainvillei	GEMARS 1472	Head	Neonate	755	Frozen	MRI/DS
Pontoporia blainvillei	GEMM 220	Head	Neonate	689	Frozen	CT/DS
Pontoporia blainvillei	GEMARS no number	Body	Perinatal	200	Formalin	MRI
Pontoporia blainvillei	MUCIN (MM36)	Body	Foetal	?/90 (F20)	Formalin	7- MRI
Pontoporia blainvillei	MUCIN (MM35)	Head	Foetal	66/54 (F20)	Formalin	7- MRI/HIS
Family Phocoenidae						
Phocoena phocoena	FTZ 1366	Head	Adult	1100	Frozen	MRI†
Phocoena phocoena	FTZ 905	Head	Adult	1615	Frozen	CT
Phocoena phocoena	FTZ 1281	Head	Subadult	1060	Frozen	MRI†
Phocoena phocoena	SNG 1903	Head	Neonate	?	Frozen	CT/MRI
Phocoena phocoena	FTZ 898	Head	Neonate	780	Frozen	MRI†
Phocoena phocoena	SAI 7613	Body	Neonate	700	Formalin	DS
Phocoena phocoena	FTZ 903	Head	Perinatal	620	Frozen	CT/MRI†
Phocoena phocoena	CN 138	Head	Perinatal	420	Frozen	CT
Phocoena phocoena	SAI (MK)76	Head	Foetal	134/60 (F22)	Formalin	HIS
Phocoena phocoena	SAI (MK)69	Head	Foetal	107/46 (C19)	Formalin	HIS
Phocoena phocoena	SAI (MK)61	Body	Foetal	95/45 (C19)	Formalin	HIS
Phocoena phocoena	SAI (MK)19	Head	Foetal	?/36 (C18)	Formalin	HIS
Phocoena phocoena	SAI (MK)62	Body	Foetal	70/28.6 (C18)	Formalin	HIS
Phocoena phocoena	SAI (MK)64	Body	Foetal	60/24 (C18)	Formalin	HIS
Phocoena phocoena	SAI (MK)70	Body	Foetal	42/18 (C16)	Formalin	HIS
Phocoena phocoena	SAI (MK)71	Head	Foetal	28/11.5 (C14)	Formalin	HIS
Family Delphinidae						
Cephalorhynchus sp.	SAI no number	Head	Adult	?	Frozen	MRI†
Tursiops gephyreus	GEMARS 1447	Head	Adult	2480	Frozen	CT/DS
Tursiops truncatus	SAI 7928	Head	Neonate	?	Formalin	CT/MRI/CS†
Stenella longirostris	SAI (PGT) 037	Head	Perinatal	761	Formalin	CT/MRI/DS
Grampus griseus	SAI (PEN) 842	Head	Perinatal	649	Formalin	7 – MRI
Stenella attenuata	SAI (RXM) 056	Head	Perinatal	550	Formalin	7 – MRI/CS
Delphinus delphis	SAI (DBH)161	Body	Foetal	432/- (F23)	Formalin	7 – MRI/CS
Delphinus delphis	SAI (TBS)199	Head	Foetal	233.81/- (F22)	Formalin	7 – MRI/HIS
Lagenorhynchus albirostris	SAI (MK)77	Head	Foetal	107/46 (C18)	Formalin	HIS

*Length of foetuses is expressed as total length/crown–rump length (mm) followed by its Carnegie/Foetal system defined by Thewissen & Heyning (2007).
†Further information on these specimens can be found in Huggenberger (2004).
CN, Zoological Museum of the University of Copenhagen, Denmark; SAI, Dr. Senckenbergische Anatomie (Department of Anatomy III, Johann Wolfgang Goethe-University, Germany; SNG, Senckenbergische Naturforschende Gesellschaft, Germany; GEMARS, Grupo de Estudos de Mamíferos Aquáticos do Rio Grande do Sul, Brazil; FTZ, Forschungs- u. Technologiezentrum Westküste, Büsum, Germany; GEMM, Grupo de Estudos de Mamíferos Marinhos da Região dos Lagos, Brazil; MUCIN, *Museu de Ciências Naturais – Universidade Federal do Rio Grande do Sul*, Brazil. Methods applied: CT, computed tomography; 7-MRI, 7-tesla magnetic resonance; MRI, magnetic resonance imaging; MD, macroscopical dissection; CS, cross section.

COMPUTED TOMOGRAPHY (CT) AND MAGNETIC RESONANCE IMAGING (MRI)

Existing CT and MRI-scan series (see Table 1) were combined with new data representing different ontogenetic stages of these three specific groups. CT-scans of further specimens were performed in the Department of Radiology of the Uniklinik, University Hospital of Cologne, Germany, resulting

in a sequence of images (1-mm slice thickness) in all three planes (i.e. coronal, sagittal and horizontal). Conventional MRI and 7-Tesla MRI-scans were performed in the Max-Planck Institute for Metabolism Research, in Cologne, Germany, using a Siemens Magnetom Prisma and a Bruker BioSpec 70/20 scanner, respectively. The CT and MRI image series were analysed using 3D-Slicer. The structures were identified using the segmentation technique (Cranford *et al.*, 2008) for which the images were edited voxel by voxel on the three planes, accomplished with a threshold assistance tool. Each fat tissue and bone structure was built as a 3D model to characterize their general topography, as well as to perform allometric comparisons. Epicranial complex length (ECL) was calculated in parallel, by using the line that passes vertically through the anterior tip of the melon and between the bursae complexes; and from point to point, from the tip of the melon to the middle point between both dorsal bursae complexes.

Gross dissection and cross-sections

The muscles and connective tissues surrounding the blowhole region were dissected, layer by layer, to describe and demonstrate the nasal soft tissues (Schenkkan, 1972). A brain-sectioning blade was used to perform horizontal cross-sections of ~10-mm slice thickness in the epicranial complex of perinatal specimens. The neonate *Tursiops truncatus* was cross-sectioned at ~20-mm slice thickness in the horizontal plane to visualize and demonstrate the arrangement of the main fat structures in the nose.

Terminology and general description

Terminology follows Klima (1999) for the early nasal cartilage in foetal specimens and Comtesse-Weidner (2007) for most early soft nasal tissues; Mead (1975), Rodionov & Markov (1992) and Huggenberger *et al.* (2014) for soft tissues in adults; and Mead & Fordyce (2009), adapted to NAV (2017), for the skull. The bauplan orientation of the foetuses follows NAV (2017). The melon (Corpus adoposum nasalis terminalis) was defined based on its main body definition (cf. Discussion). Precursor tissues of the main structures involved in sound production such as the dorsal bursae complex, the rostrum and facial skull, the nasal diverticula, melon and the branches of the melon, connective tissue theca, etc., were identified by comparing the topographical position and composition of the structures as found in adults. Some important structures such as the phonic lips (Valva nasalis intermedia) were not examined due to sample fixation. Foetal tissues were described to elucidate the development and formation of the mature, well-known general adult morphology (see references in Discussion).

Phylogenetic approach

The main developmental changes in the soft nasal tract in dolphins were used to create transformational characters (de Pinna, 1991) as proposed by Fink (1982) (see Supporting Information, File S1), in which, theoretically, ordered states represented ontogenetically based transformations and, thus, state transformation and reversions were considered heterochronic changes. Conventional characters were also created with non-ontogenetically based transformations, and additional descriptions were compiled from the literature to represent the morphological variation among odontocetes. All seven characters were constructed following Sereno (2007) and added to the list of Peredo *et al.* (2018), which is a modified version of Lambert *et al.* (2017). We included the new data (Supporting Information, File S2) using the matrix of Kimura & Hasegawa (2019), which added a new taxon into the supermatrix. Phylogenetic analysis was conducted with TNT software (Goloboff *et al.*, 2008) using the New Technology Search with default values, except that the application was tasked to find the shortest trees 1000 times. The consistency index (CI) and retention index (RI) of each added character and Character 100 of Lambert *et al.* (2017) were calculated and are shown in the character description. The morphology of extinct groups was inferred using the parsimony method for ancestral character reconstruction (File S1) in Mesquite v.3.40 (Maddison & Maddison, 2018). Developmental processes in heterochronic terms were classified according to Gould (1977) and Alberch *et al.* (1979), as summarized by Klingenberg (1998).

RESULTS

General features of foetal development of the soft nasal structures

The morphogenesis of the soft nasal tissues in dolphins was remarkable for its transformation early in ontogeny: the smallest foetal analysed (MK 71, *Phocoena phocoena*, crown–rump length = 11.5 mm, Carnegie stage C14) presented a loose-like connective tissue containing mesemchymal cells with a large amount of intercellular substance dorsally (future posteriorly, see below) to each foetal nasal passage and surrounded by undifferentiated cells anteriorly and posteriorly (Fig. 1A, B). On its ventral portion (future anterior portion, see below), the foetal nasal passage exhibited more heterogeneous tissue, primarily being

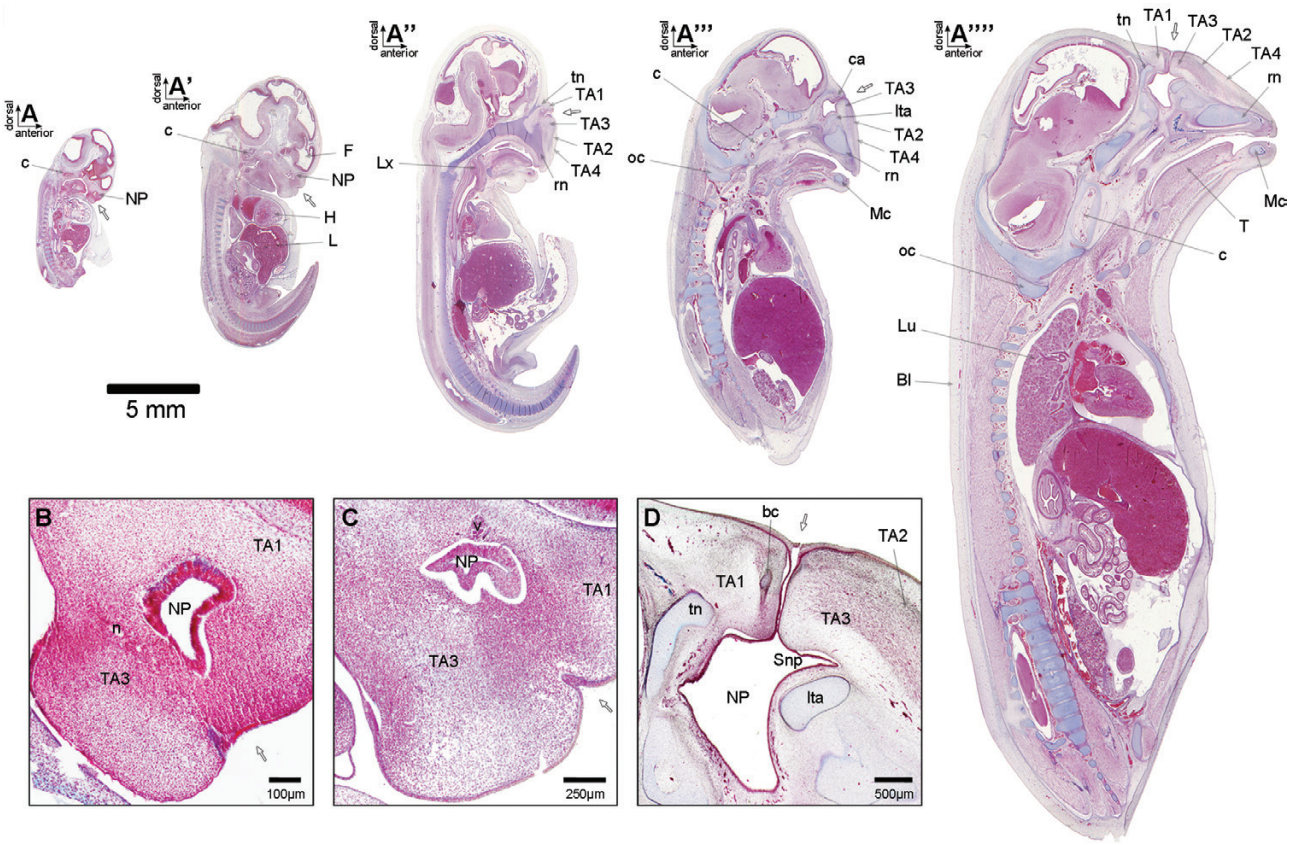

Figure 1. Early development of *Phocoena phocoena* in sagittal section. A, MK 71 crown–hump length = 11.5 mm, Carnegie stage 14. A', MK 70 crown–hump length = 18 mm, Carnegie stage 16. A", MK 64 crown–hump length = 24 mm, Carnegie stage 18. A"', MK 62 crown–hump length = 28.6 mm, Carnegie stage 18. A"", MK 61 crown–hump length = 45 mm, Carnegie stage 19. B, MK 71. C, MK 70. D, MK 61. Abbreviations: bc, bursae cartilage; Bl, blubber precursor tissue; c, cochlea; ca, cupula nasi anterior cartilage; F, forebrain; H, heart; L, liver; lta, lamina transversalis anterior cartilage; Lx, larynx; Lu, lungs; Mc, Meckelian cartilage; n, nerve; NP, nasal passage; rn, rostrum nasi cartilage; oc, occipital condyle; T, tongue; tn, tectum nasi cartilage; v, vessel. For TA1 to TA4, see main descriptions. External nasal passage positions are indicated by white arrows.

composed of undifferentiated mesenchymal cells along its ventral surface and lightly stained cells with brighter nuclei at the anterior tip of the face. Undifferentiated mesenchymal cell at a point just below the ventral surface of each foetal nasal passage showed cells divided by intercellular substance and a few collagen fibres, which ran downwards, and anteriorly over the loose-like connective tissue at the tip of the rostrum. This was also observed in the slightly larger foetus MK 70 (*Phocoena phocoena*, crown–rump length = 18 mm, Carnegie stage C16) (Fig. 1A', C). At this stage, the external nares were separated into two nasal passages by the septum nasi (sn) (see Fig. 3), which reached the distal portion of the nasal apertures, and was positioned at the snout tip (not shown in the figures). The primitive nasal passages were aligned horizontally to the septum nasi and both sides had a symmetrical tissue organization.

FOETAL TISSUE MATURATION

Ontogenetic changes were observed between Carnegie stages C16 and C19 in *Phocoena phocoena* specimens as body curvature changed slightly from the typical 'C' shaped form to a less concave condition. The head streched relative to the body axis; and the posterior portion of the body changed its orientation as observed by the alignment of the lumbar vertebrae with the main axis of the body in late Carnegie stage C18 specimens (Fig. 1). In all specimens classified as Carnegie stage C18 (MK 62, MK 64, MK 77), the nasal cartilage developed anteroventrally by elongation of the rostrum nasi (rn); and dorsally (i.e. to the vertex of the skull) by the tectum nasi (tn) and projections of the cupula nasi anterior (ca) (see below) (Fig. 1A", A"', A""). At this stage, the external nasal passages became

adjacent to each other via anterodorsal extension of the cartilagenious cupula nasi anterior. Thus, this cartilage, which surpassed the level of the septum nasi, sustained the associated soft tissue dorsally/posteriorly positioned relative to each nasal passage (Figs 1A"", A"", 2). The loose connective tissue dorsal/posterior to each nasal passage (herein topographical area 1, TA1) was surrounded by another tissue composed of a line of mesenchymal cells. The latter streched from the projections of the cupula nasi anterior between

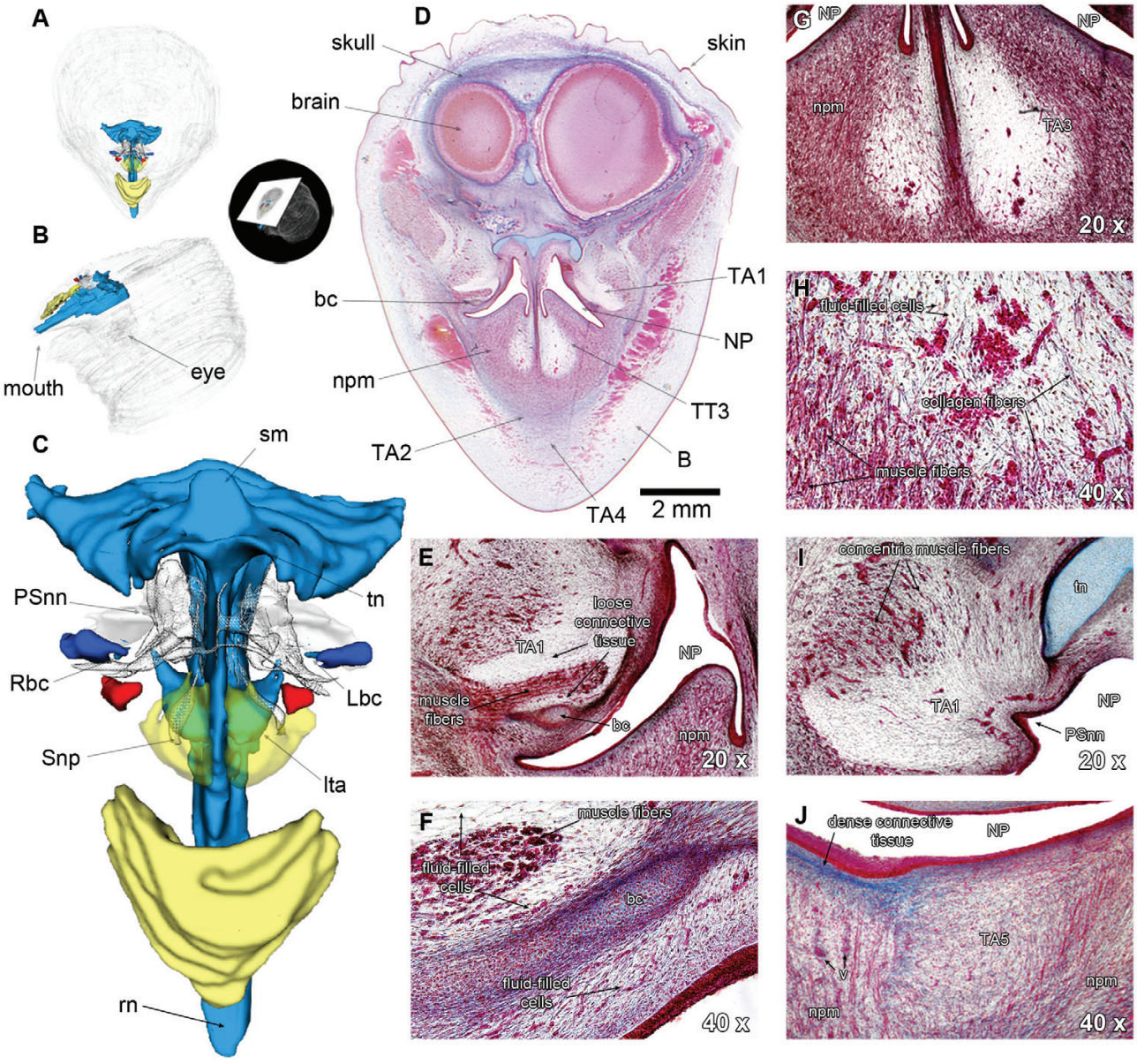

Figure 2. Anatomy of the nasal structure precursor tissues in a late *Phocoena phocoena* foetus (MK 76, total length = 134 mm, Carnegie stage F22). A–C, 3D reconstructions from histological slides; D–J, demonstrating general head (translucent white) and nasal cartilages (cyan) morphology, including the bursae cartilage (bc). The main precursor tissues and structures of the sound production apparatus were labelled in 3D (C) (anterior dorsal bursae, red; branches of the melon, translucent yellow; loose connective tissue covering the posterior Snn, white; melon, yellow; nasal passage (NP) and nasal air sacs, white wireframe; posterior dorsal bursae, blue) and demonstrated by focal microscopy photographs (E–J). Abbreviations: B, blubber precursor tissue; lta, lamina transversalis anterior cartilage; Lbc, left bursae cartilage; npm, nasal plug muscle; PSnn, posterior Saccus nasalis nasofrontalis; Rbc, right bursae cartilage; rn, rostrum nasi cartilage; sm, spina mesethmoidalis; Snp, saccus nasalis praemaxillaris; tn, tectum nasi cartilage; v, vesssel. For TA1 to TA5, see main descriptions.

Carnegie stages C16 and C18, running distally and posteriorly while muscle and collagen fibres started to grow concentrically in parallel (e.g. Figs 1D, 2E, I).

The anterior portion of the primitive epicranial complex exhibited undifferentiated mesenchymal cells (herein topographical area 2, TA2) at Carnegie stages C16 and C19 extending from the lips of the blowhole (Valva nasalis dorsalis) to a point between the rostrum nasi tip and its midline, where it reaches the loose appearing connective tissue covering the dorsal surface of the rostrum nasi (Fig. 1A"). The TA2 dorsally covered the heterogeneous loose connective tissue positioned just below/anterior to the nasal passage (herein topographical area 3, TA3), dividing the anterior portion of the primitive epicranial complex in TA3 posteriorly/below and a loose connective tissue (herein topographical area 4, TA4) rostrally. At these stages, TA4 resembled the blubber precursor tissue found around the foetus body (Fig. 1A"'), i.e. composed of light cells with large vacuoles below the epidermis. Increasing collagen fibres within fibroblasts horizontally orientated relative to the axis of the rostrum nasi appeared in TA4 at late Carnegie stage 18 – as was observed in *Phocoena phocoena* (MK 62, crown–rump length = 28.6 mm) and *Lagenorhynchus albirostris* (MK 77, crown–rump length = 46 mm). It dorsally covered the premaxillary (os incisivum, OI) and maxillary (M) bones, i.e. their anterior portions. In all specimens classified as Carnegie stage 18, including *L. albirostris*, muscle fibres from the Musculus maxillonasolabialis rostralis (mr) – or Musculus maxillonasolabialis partes profundus, lateralis et medialis in adults – were observed attached to TA4, laterally on both sides of the primitive epicranial complex. The fibres extended from the anterior portion of the premaxillary and maxillary bones to the posterior end of the maxillary bone, which was positioned posteriorly to the nasal passage and rostrolaterally to the braincase (Fig. 2).

Interspecific variation was noted in late foetal development, although no direct comparisons were possible between each of the Carnegie stages of all three studied odontocete groups. The main difference was in the size and proportions of the rostrum nasi cartilage, which was prominent in Carnegie stage F20 in *Pontoporia blainvillei* compared to later stages in *Delphinus delphis* and *Phocoena phocoena* (Fig. 3), reaching almost three times the braincase width in *Pontoporia blainvillei*. *Pontoporia blainvillei* was the only species exhibiting a rostrum surpassing the anterior limits of the epicranial complex during foetal stages. However, the epicranial complex remained similar in composition and proportion compared to the other species, except in the size of the invaginations of the nasal complex. These invaginations became relatively larger from stage to stage (Fig. 4).

Bony tissues were detected for the first time, ontogenetically, in Carnegie stage C18 specimens: MK 64 (*Phocoena phocoena*, crown–rump length = 24 mm) was the smallest specimen presenting bone formation. It was only found in the head region, i.e. in the frontal bone (os frontale, OF), originating posteriorly to the lateral tip of the septum interorbitale (si) and running

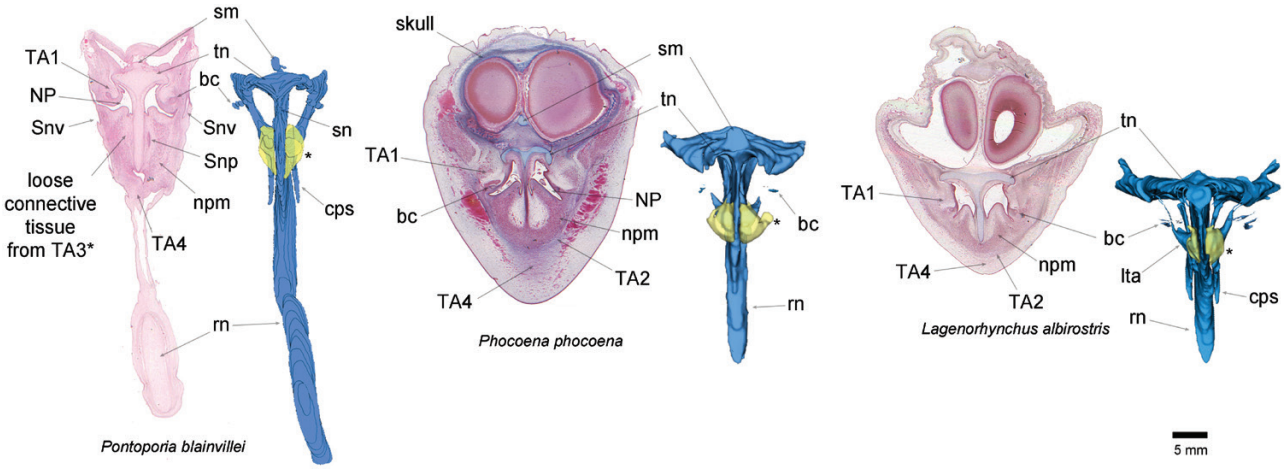

Figure 3. 3D reconstructions from histological slices of the nasal cartilages (cyan) and the loose connective tissue from TA3 (translucent yellow) in late foetuses of *Pontoporia blainvillei* (MM 35, crown–hump length = 54 mm, Carnegie stage F20), *Phocoena phocoena* (MK 76, total length = 134 mm, Carnegie stage F22), and *Lagenorhynchus albirostris* (MK 77, crown–hump length = 46 mm, Carnegie stage F18) in dorsal view. Abbreviations: bc, bursae cartilage; cps, cartilago paraseptalis; lta, lamina transversalis anterior cartilage; NP, nasal passage; npm, nasal plug muscle; rn, rostrum nasi cartilage; Snp, Saccus nasalis praemaxillaris; Snv, Saccus nasalis vestibularis; sm, spina mesethmoidalis; sn, septum nasi cartilage; tn, tectum nasi cartilage. For TA1 to TA5, see main descriptions.

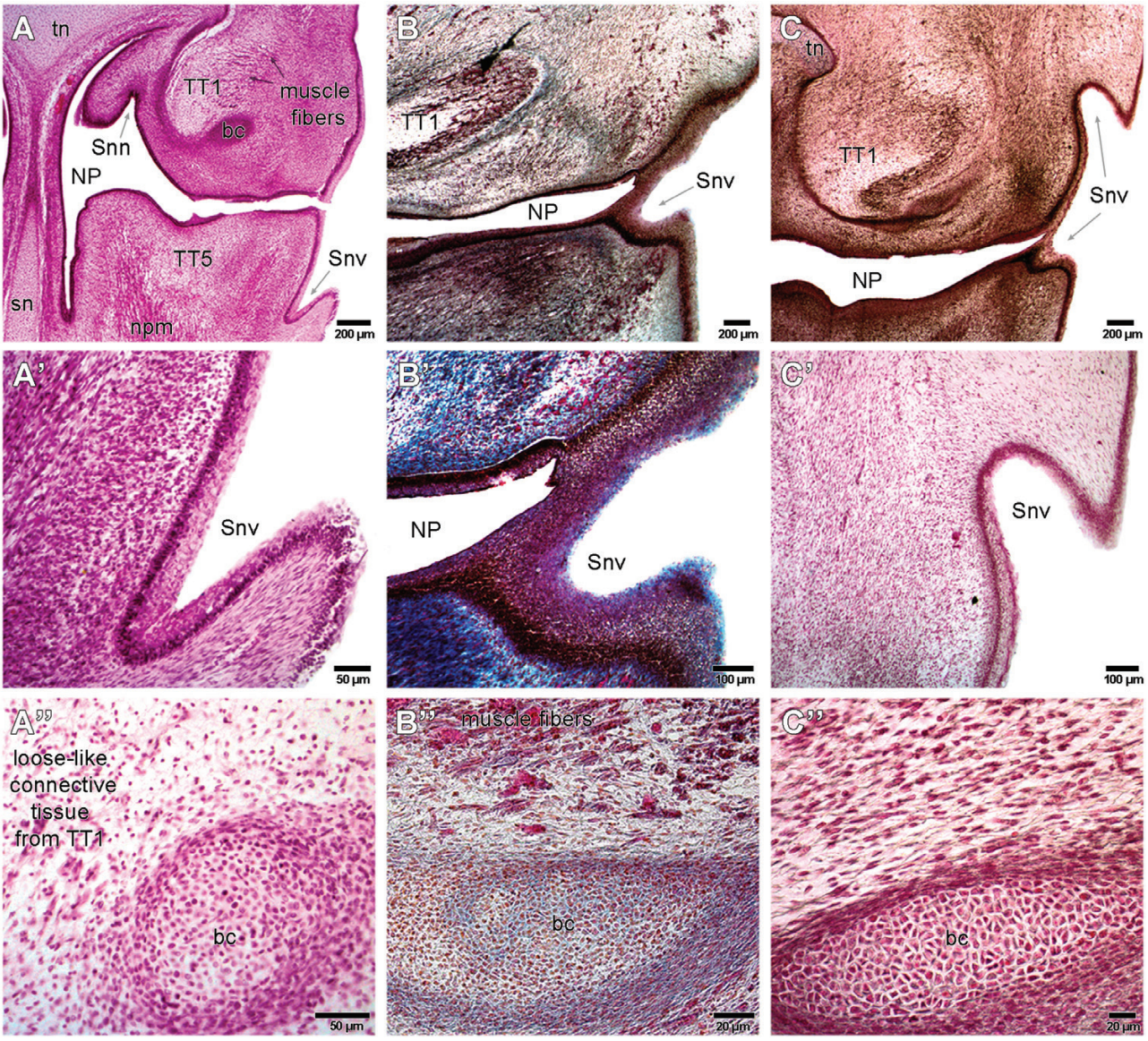

Figure 4. Histological sections of the primitive epicranial complex in (A, A', A") *Pontoporia blainvillei* (MM 35, crown–hump length = 54 mm, Carnegie stage F20), (B, B', B") *Phocoena phocoena* (MK 76, total length = 134 mm, Carnegie stage F22) and *Lagenorhynchus albirostris* (C, C', C") (MK 77, crown–hump length = 46 mm, Carnegie stage F18), in dorsal view, demonstrating the early formation of the vestibular air sacs (Saccus nasalis vestibularis, Snv) (A, A', B, B', C, C'), and interespecific morphological variation of the bursae cartilage (bc) (A", B", C"). Abbreviations: NP, nasal passage; Snn, Saccus nasalis nasofrontalis; sn, septum nasi cartilage; Snv, Saccus nasalis vestibularis; npm, nasal plug muscle.

dorsolaterally while covering both sides of the anterior forebrain (not shown in figures). The maxillary bone presented ossification at its posterior portion just in front of the frontal bone (i.e. posterior to the nasal passage), building an ossified plate on both sides of the septum nasi with little bony tissue surrounding the rostrum nasi, posteriorly. The premaxillary bone originated from both sides of the lamina transversalis anterior cartilage (lta) and extended anteriorly through the rostrum nasi while surpassing the anterior limits of the ossified portion of the maxillary bone. The mandibula (Ma) laterally covered the Meckel's cartilage from a line that passes vertically through the eye, posteriorly, and extending to the tip of the Meckel's cartilage anteriorly. In foetal stages, the septum nasi was a thin cartilage surrounded by the maxillary and premaxillary bones, posteriorly. In *Phocoena phocoena*, the inner ear started ossification later than the nasal structures, at early Carnegie stage C19, by the tympanic bone (os tympanicum) characterizing the morphogenesis of the tympanic cavity.

The connective tissue of the topographical areas (TAs) at early stages in *Phocoena phocoena* (Figs 1, 2) was topographically positioned in the same regions of the primitive epicranial complex as in the other studied species. The TA3 in late foetal stages (i.e. Carnegie stages F20 to F22) consisted of concentric muscle and collagen fibres anterior to each nasal passage between the deepest nasal invagination – placed just above the lamina transversalis anterior cartilage – and the TA2, which covered the epicranial complex dorsally (Figs 2, 3). The composition of TA3 showed a clear association with the nasal cartilage, specifically with the dorsal portion of the septum nasi: the heterogeneous composition of this tissue was due to the loose connective tissue composed of lightly stained mesenchymal cells with round nuclei. These cells were disposed in a matrix supported by dense extracellular substances coloured in blue and irrigated by blood vessels (Fig. 2). The shapes of these loose connective tissue structures varied between species and ontogenetic stages because they became elongated in early stages such as in *L. albirostris* (MK 77, crown–rump length = 46 mm, Carnegie stage C18) and in *Pontoporia blainvillei* (MM 35, crown–rump length = 54 mm, Carnegie stage F20). Here, they laterally surrounded the septum nasi and dorsally covered the lamina transversalis anterior cartilage and the deepest nasal invaginations (Fig. 2). In late-stage foetuses, such as in *Phocoena phocoena* (MK 76, total length = 134 mm, Carnegie stage F22) and *D. delphis* (TBS 199, total length = 233.81 mm, Carnegie stage F22), the septum nasi was reduced to a thin cartilage that separated both right and left TA3s, which comprised loose connective tissues embedded into concentric collagen and muscle fibres of the TA3 (Figs 2–4). Additionally, in the late-stage *D. delphis* (TBS 199), the loose connective tissue from TA3 exhibited increased collagen and muscle fibres from the nasal plug muscles (npm).

Dorsolaterally of each TA3 and placed just anteriorly to the nasal passage at the distal border of the nasal diverticula, a pair of small loose connective tissue structures (herein topographical area 5, TA5) were found from Carnegie stage C19 onwards (Fig. 2). These structures exhibited similar arrangements to those found in TA3, with dense extracellular matrix sustaining the light stained cells (Fig. 4A). In the late-stage *D. delphis* (TBS 199) foetal, both TA5 exhibited increased collagen fibres. Anteriorly, TA5 was attached by the axially oriented collagen and muscle fibres originating from TA3 and was surrounded dorsally by the TA2 and ventrally by a dense connective tissue that covered the anterior portion of the nasal passage. The TA2 was primarily composed of dense collagen and muscle fibres disposed concentrically around TA3 at later foetal stages (i.e. F20 to F22) in all three groups. The collagen fibres were attached ventrally to a thin and oblique membrane of connective tissue between the anterior portion of the lamina transversalis anterior and the rostrum nasi cartilages, just at the rostrum base, and dorsally at the blowhole ligament.

Major changes in *Phocoena phocoena* between Carnegie stages C16 to C18 included the blubber differentiation that covered the whole body of the foetus, which coincided with the anterior development of the rostrum nasi and the displacement of the external naris towards the top of the head (Fig. 1A–A""). Simultaneously, in *Phocoena phocoena* (MK 76, Fig. 2), TA4 originated ventrally from the loose connective tissue covering the dorsal surface of the rostrum nasi tip, where collagen fibres concentrically converged from each side of the cartilage connecting anterior muscle fibres from each side of the Musculus maxillonasolabialis rostralis. The concentric collagen fibres from TA4 were thicker just anterior to the primitive epicranial complex, where the fibres extended horizontally from both sides of the blubber precursor tissue anchoring the medial portion of the Musculus maxillonasolabialis rostralis. The collagen fibres ended dorsally at a line intersecting the level of both loose connective tissues in the TA3 and the dorsal tip of the spina mesethmoidalis. A few fibroblasts and muscle fibres from the Musculus maxillonasolabialis rostralis were embedded within the loose connective tissue of the blubber precursor tissue covering TA4 dorsally. Additionally, TA4 showed a gradually changing composition, with strong collagen fibres found close to TA2 posteriorly, while these fibres decreased in number and size rostralwards where TA4 reached the blubber precursor tissue (Fig. 2D).

The nasal cartilages were increasingly surrounded by osteological tissues from Carnegie stage C19 onwards, except the dorsal and lateral projections of the cupula nasi anterior (Figs 1A", A", A"", 2): all foetuses classified as between Carnegie stages C18 to F23 presented cartilage projections sustaining the loose connective tissue posterior to both sides of the nasal passage (i.e. TA1). These cartilages (bc) (Fig. 4A", B", C") were connected to the cupula nasi anterior by their medial portion, as mentioned before. It extended ventrally (i.e. in parallel to the nasal passage) as a cylinder through the anterior portion of TA1, ending sharply at its anteroventral portion. Below and attached to each of those cartilages, a pair of undifferentiated mesenchymal cell tissues ran ventrally (laterally within the epicranial complex) and followed the diverticula into the distalmost portion of the premaxillary air sacs, at the posterior portion of the premaxillary bones. These cartilages anchored concentric muscle and collagen fibres inserted into the loose connective tissue of TA1, while anchoring a small portion of loose connective tissue (blue structure in Fig. 2C, becoming the posterior dorsal bursae, see below) on its dorsal half. Posteriorly, it was surrounded by muscle fibres from the Musculus maxillonasolabialis. In the late foetus that we analysed histologically

(*D. delphis* – TBS 199, total length = 233.81 mm, Carnegie stage F22), the connective tissue linking the above-mentioned cartilage (bc) to the cupula nasi anterior was reduced to a thin layer of fibroblast cells, and the Musculus maxillonasolabialis had an increased number of muscle fibres posterior to TA1.

Development of nasal diverticulae

Morphogenesis of the nasal air sacs was detected during foetal development, starting at Carnegie stage 18 (Figs 1D, 2C, I). Formation of the premaxillary air sacs (Saccus nasalis praemaxillaris, Snp) was characterized by two invaginations of the nasal passage epithelium that dorsolaterally covered each lamina transversalis anterior cartilage on both sides of the epicranial complex at early Carnegie stage C18 (although it appears to be a cylindrically rostrally-orientated air space in the 3D model in Fig. 2C due to distortions between histological slices). At this stage, the nasofrontal air sacs (Saccus nasalis nasofrontalis, Snn) were detected as a pair of lateral bifurcated invaginations, in which the anterior portion was positioned anteriorly to the ventral portion of TA1. The posterior portion was smaller and exhibited associated collagen and muscle fibres from the posterior portion of TA1. The premaxillary air sacs of foetal specimens from Carnegie stages C19 to F20 exhibited an increase in relative size, but their anterior position was still dorsal to the lamina transversalis anterior cartilage. At this stage, the nasal passage was positioned more posteriorly compared to earlier stages. Additionally, the posterior portion of the nasofrontal air sacs increased relatively in size in foetal specimens of Carnegie stages F20 to F22 as it extended posteriorly and distally (i.e. laterally) as in the late *D. delphis* foetus (TBS 199, total length = 233.81 mm, Carnegie stage F22), thus surrounding TA1 posteriorly (not shown in images). Morphogenesis of the vestibular air sacs (Saccus nasalis vestibularis, Snv) was detected between Carnegie stages C18 to F22 as invaginations of the epidermis at both lateral sides of the blowhole (Fig. 4). Thus, they formed the distalmost diverticula in the dolphin head. The timing of development of the vestibular air sacs varied between the three groups analysed: in *Phocoena phocoena* it started to differentiate late in Carnegie stage F22 onwards while in *L. albirostris* (MK 77), at Carnegie stage C18, the pair of vestibular air sacs were present forming small invaginations from the epidermis at the future blowhole. In *Pontoporia blainvillei* (MM 35), the vestibular air sacs were larger than in the other specimens as they extended posteriorly and anteriorly to the nasal passage, covering the lateral sides of the epicranial complex just at the level of the bc. Although a similar condition was found in *Phocoena phocoena* and *L. albirostris*, their vestibular air sacs did not extend anteriorly to the nasal passage.

Perinatal development of the soft nasal structures

The perinatal development of the soft nasal structures was characterized by topographic and compositional changes in the epicranial complex, and were remarkably distinct between the three groups analysed in this study. Nevertheless, perinatal specimens exhibited similar general features to those found in adults, such as the straight alignment of the rostrum with the axial skeleton, complete skin pigmentation and a similar arrangement of the structures involved in sound generation (except for the monkey lips at the Valva nasalis intermedia). In delphinids, asymmetry of the epicranial complex was perceived by the larger size of the right nasal plug muscle and the right dorsal bursae complex, which was larger and was positioned more dorsally compared to the left one in all species analysed (Table 1; Fig. 5). In the following, the main soft nasal structures and their respective topographical/compositional correspondence with early foetal tissues are described.

Posterior dorsal bursae (Corpus adiposum nasalis posterior, Canp)

This pair of small ellipsoidal fat bodies was positioned just posteriorly to each nasal passage, below the vestibular air sacs and surrounded posteriorly by the nasofrontal air sacs. In the early perinatal *D. delphis* (DBH 161, total length: 432 mm), the posterior dorsal bursae complexes were associated with the loose-like connective tissue found anteriorly in each bc in TA1 in late foetal specimens (Figs 2C, F5).

Anterior dorsal bursae (Corpus adiposum nasalis anterior, Cana)

This pair of small ellipsoidal fat bodies was positioned just anteriorly to each nasal passage, surrounded by a thin and dense connective tissue, just dorsally to the nasal plug (Vnv) and the nasal plug muscles (npm) (see below). Dense collagen and muscle fibres from the npm border were located anteriorly to each anterior dorsal bursae (Fig. 5A), in a similar condition as the loose connective tissue described as TA5 in late foetal specimens (Fig. 2J).

Nasal plugs (Valva nasalis ventralis, Vnv) and nasal plug muscles (Musculus maxillonasolabialis, pars valvae nasalis ventralis, npm)

The nasal plug was characterized by dense connective tissue covering the nasal passage from anteriorly in the epicranial complex, just below the anterior dorsal bursae and dorsally to the premaxillary air sacs. The topographical position of the nasal plug resembled the growing dense connective tissue found at the same

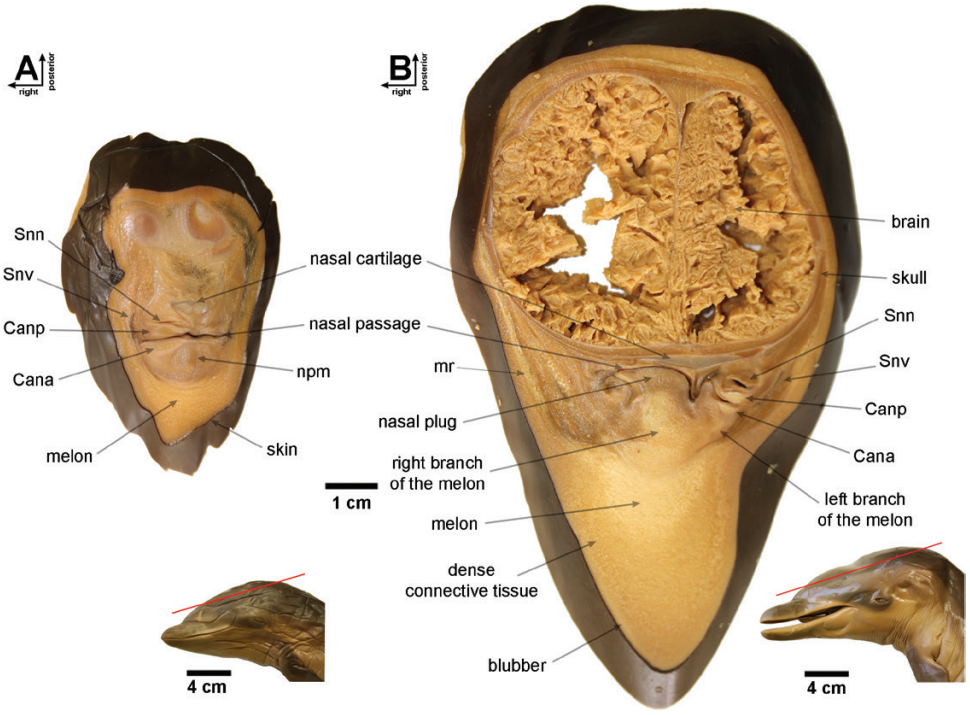

Figure 5. Soft nasal structures in perinatal delphinid specimens. A, *Delphinus delphis* (DBH 161, total length = 43.2 cm); B, *Stenella longirostris* (PGT 037, total length = 76.1 cm). Cana, anterior dorsal bursal (Corpus adiposum nasalis anterior); melon, Corpus adiposum nasalis terminalis; mr, Musculus maxillonasolabialis rostralis; npm, nasal plug muscle (Musculus maxillonasolabialis, pars valvae nasalis ventralis); Snn, nasofrontal air sac (Saccus nasalis nasofrontalis); Canp, posterior dorsal bursae (Corpus adiposum nasalis posterior); Snv, vestibular air sacs (Saccus nasalis vestibularis).

position in late foetuses (Fig. 2D, G, J). The nasal plug muscle showed remarkable variation during perinatal development among the three groups analysed. In the investigated delphinids, the right-hand side nasal plug muscle became larger and composed of dense and concentric muscle fibres surrounding two small fatty tissue structures that extended posteriorly from the nasal passage to the concentric muscle fibres of the Musculus maxillonasolabialis, anteriorly (Fig. 5). The muscle arrangement of the nasal plug resembled TA3 found in foetal specimens based on the topographical position of both tissues. Moreover, in delphinids, the muscle fibres from the nasal plug muscles were disposed in the same orientation as in TA3, while the fat pathways, which can be described as branches of the melon, were placed on both sides of the epicranial complex. These branches were embedded in the muscle and collagen fibres of the nasal plug muscles and were topographically positioned at the same position as the loose connective tissue found in TA3 during foetal development (Figs 2, 3).

Despite the clear asymmetry of the nasal plug and the nasal plug muscles during perinatal development in delphinids, promoted by the earlier timing of development of the right portion of these structures, major differences in the composition of the nasal plug muscles were found between the three groups analysed. In delphinids, the right nasal plug muscle was expanded by an increasing number of collagen and muscle fibres with a large amount of fat between the layers (right branch of the melon, rm). In comparison, the left branch of the melon (lm) (Fig. 5), positioned just ventrally to the anterior dorsal bursae and surrounded by collagen and muscle fibres, was much smaller. In delphinids, the Musculus maxillonasolabialis was embedded in the fat tissue, thus forming a continued fat pathway from the anterior portion of the nasal passage into the melon, as seen in adults (see below). In *Phocoena phocoena*, the nasal plug muscles were nearly symmetrical tissues composed of dense collagen and muscle fibres on each side of the epicranial complex, and there was no evidence of fat tissues within the fibres. In *Pontoporia blainvillei*, the nasal plug muscles were also nearly symmetrical and composed of collagen and muscle fibres surrounding fat tissues on both sides, as seen in adults (see below).

Melon (Corpus adiposum nasalis terminalis, melon)

The largest fat tissue structure in the dolphin head was composed of concentrically orientated collagen

fibres, anchored on both sides of the medial portion of the Musculus maxillonasolabialis rostralis (mr), with a large amount of adipose tissue between the layers (Fig. 5). Late perinatal specimens exhibited increased adipose tissue between the collagen fibres and started to shape the rounded curvature of this structure (Fig. 5B). The melon (Fig. 5) clearly resembled the TA4 described in foetal stages (Figs 1–3).

Nasal diverticulae

The nasal diverticula exhibited continued topographical transformation due to formation of the vestibular air sacs and the nasofrontal air sacs, while the premaxillary air sacs presented a similar shape to that of adults during perinatal development. The pair of premaxillary air sacs was positioned at both posterior projections of the premaxillary bones as observed in late foetal specimens. They extended from the nasal passage to the anterior border of the nasal/posterior portion of the premaxillary bones. They were thus asymmetric in the investigated delphinids, while in *Phocoena phocoena* and *Pontoporia blainvillei* they were nearly symmetric. The nasofrontal air sacs originated on the posterior wall of the nasal passage, surrounded posteriorly by connective tissue at the position of TA1 in early foetuses (Figs 2–5). In the early perinatal *D. delphis* (DBH 161, total length = 432 mm), the nasofrontal air sacs were not pigmented. In delphinids and *Phocoena phocoena*, it developed anteriorly while surrounding the nasal passage and the anterior dorsal bursae, while in *Pontoporia blainvillei*, the anterior portion of the nasofrontal air sacs was absent. In *Phocoena phocoena* and *Pontoporia blainvillei*, the connective tissue surrounding the posterior portion of the nasofrontal air sacs has differentiated to a dense and rigid connective tissue composed of concentric fibres on each side of the nasal passage.

The pair of vestibular air sacs was the distalmost invagination of the nasal passage, starting at the early foetal blowhole slit and present in all perinatal specimens. In the perinatal *D. delphis* (DBH 161), the vestibular air sacs covered dorsally and laterally the posterior dorsal bursae complex with shallow invaginations at its anterior portion. These invaginations were more pronounced in larger perinatals such as in *Stenella longirostris* (PGD 037, total length = 761 mm). In this specimen, the vestibular air sacs showed this feature in the whole structure. In late *Phocoena phocoena* perinatals – such as SAI 7613 (total length = 700 mm) – the vestibular air sacs were the largest structure in the epicranial complex (except for the melon), and exhibited a higher degree of invaginations.

Postnatal development of the soft nasal structures

At birth, all specimens exhibited all structures involved in the sound generation process. However, despite allometric changes related to the increased size (Supporting Information, File S3), topographical and compositional transformations occurred during postnatal development of the epicranial complex (Figs 6, 7) as the final steps to a mature (i.e. adult looking) sound-generating apparatus. Topographical changes of the epicranial complex occurred in parallel to skull formation. The posterior portion of the premaxillary bone exhibited great variation among the species analysed. In *Pontoporia blainvillei* and *Phocoena phocoena*, the elevation of the dorsal surface of the posterior (nasal) portion of this bone during postnatal development directly elevated the premaxillary air sacs and all the soft nasal tissues positioned anterior to the nasal passage in relation to the length axis of the skull (Fig. 7). In these species, the posterior and anterior dorsal bursae were aligned with the posterior portion of the main body of the melon along this length axis (Fig. 7). In *Tursiops* spp., the posterior (nasal) portion of the premaxillary bone was concave and lacked major shape transformations during postnatal development.

The bursae complex (i.e. right and left anterior dorsal bursae and right and left posterior dorsal bursae) presented similar allometric changes (Supporting Information, File S3), and in their relative position in the three groups analysed, because in all neonatal specimens, the posterior dorsal bursae were dorsocaudally positioned relative to the anterior dorsal bursae while they were aligned axially in adults (Fig. 7). The caudal movements of both posterior portions of the maxillary and premaxillary bones and associated facial muscles plus connective tissues resulted in a topographical rearrangement of these structures relative to the bursae complex in adults. The steeper vertex of the skull in *Tursiops* spp. reflected the distinct arrangement of the posterior melon in most delphinids: the right branch of the melon extended posteriorly while following the shape development (Fig. 7). In *Pontoporia blainvillei*, the dorsal movement of the posterior (nasal) portion of the premaxillary bone, described above, and the caudal movements of the maxillary and the nasal bones resulted in a flattened dorsal surface of the adult skull, serving as the base of the epicranial complex (Fig. 8A). Additionally, adult *Pontoporia blainvillei* displayed an elongated right branch of the melon compared to the neonate (Figs 6, 7).

The rostrum developed in three distinct group-specific ways: in delphinids, the rostrum developed anteriorly and increased in size relative to the melon (Supporting Information, File S3) while the melon exhibited less convexity of its anterior portion in adults compared to

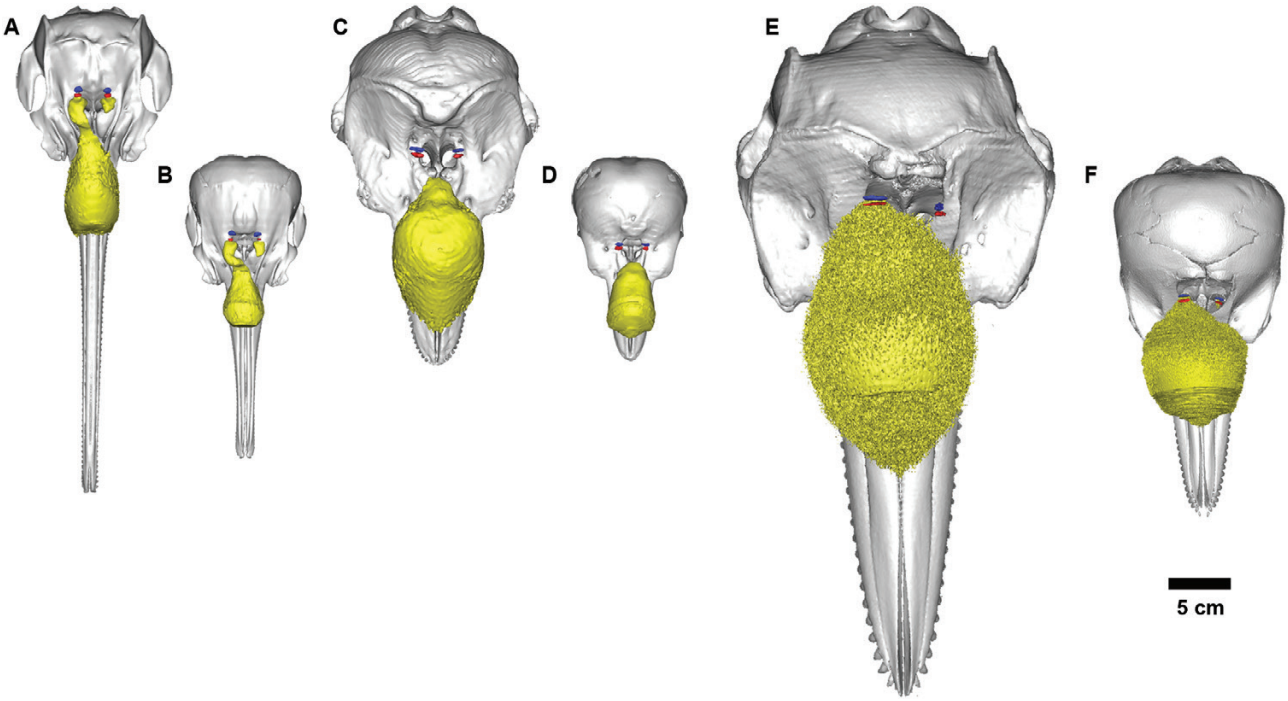

Figure 6. 3D reconstructions of the main fat pathways (posterior dorsal bursae, blue; anterior dorsal bursae, red; melon and the branches of the melon, yellow) and the skull of *Pontoporia blainvillei* (A, B), *Phocoena phocoena* (C, D) and *Tursiops* spp. (E, F) in dorsal view.

neonates (Fig. 7). In *Pontoporia blainvillei*, the rostrum developed slightly anteroventrally, while presenting a more convex dorsal surface, also apparent in the anterior shape of the melon. In *Phocoena phocoena*, the rostrum and the melon presented a constantly similar shape and relative size throughout postnatal ontogeny. Compositional changes were observed during the postnatal development of the left branch of the melon (lm) in *Tursiops* spp.: the neonate specimen analysed, as also observed in all perinatal delphinids, presented a fat pathway ending in the nasal plug just below (ventral) the left anterior dorsal bursae. In the adult, the left nasal plug was composed of dense connective tissue with concentric collagen fibres (Fig. 8C, D). By contrast, *Phocoena phocoena* did not exhibit the right and left branches of the melon, but instead in their relative position concentric dense collagen fibres and muscle fibres (Fig. 8B). The ontogenetic dorsal movement of the posterior portion of the premaxillary bones elevated the left premaxillary air sacs and changed the orientation of the left branch of the melon to a more anterodorsal alignment relative to the axis of the skull in *Pontoporia blainvillei* and *Phocoena phocoena* (Fig. 7).

Phylogenetic analysis

Seven new characters (325 to 331) represented the main features related to the directional properties of the sound production in odontocetes (Aroyan *et al.*, 1992; Au *et al.*, 2010; Wei *et al.*, 2017). Phylogenetic analysis resulted in four shortest trees with a length of 4 565 997 steps, a CI of 0.587 and an RI of 0.498. Independent changes in ontogenetic patterns of the sound-generating structures in odontocetes led to morphological diversity of biosonar designs found in this group. The evolution of the vestibular air sacs (trait only) (Character 100, Supporting Information, File S1) may have two explanations. (1) Acceleration of the formation of the tissues surrounding the blowhole between Carnegie stages C18 and F22 could have evolved independently in Physeteroidea and Delphinida (i.e. homoplasic condition). (2) By contrast, these changes in blowhole formation at foetal stages might have evolved in a common ancestor of crown cetaceans, and consequently, paedomorphic (post-displacement) events might thus have occurred in a common ancestor of Ziphiidae and Platanistidae for its loss (File S1).

Although rostrum size, relative to the epicranial complex length (ECL) (Character 330, Supporting Information, File S1), may have evolved under more than one heterochronic process (e.g. rostrum increased/decreased and increasing melon development), we perceived that, within Delphinida, the decreased size of the rostrum relative to the ECL supports the Delphinoidea clade: Delphinidae + (Phocoenidae + Monodontidae).

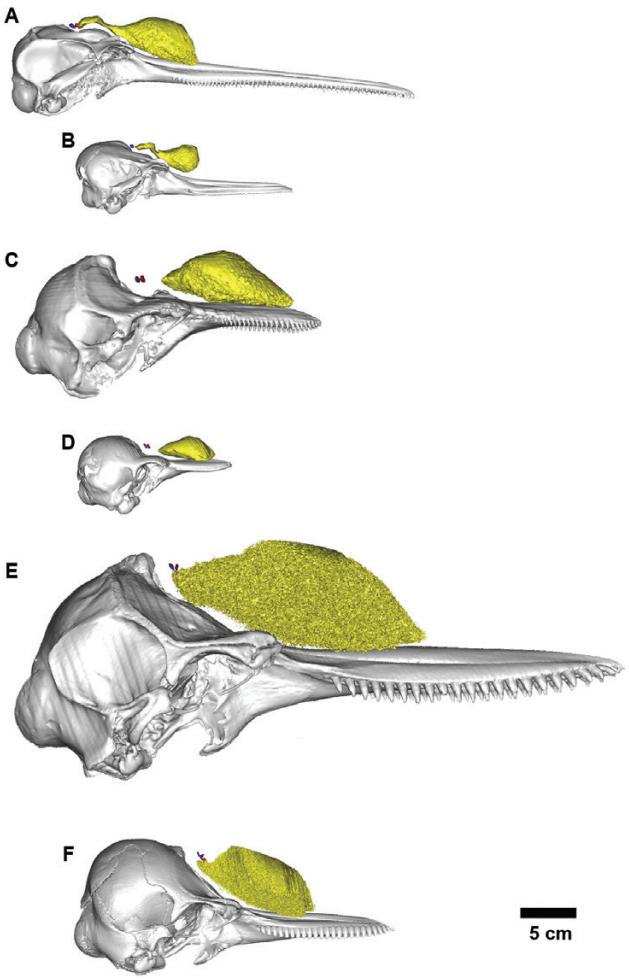

Figure 7. 3D reconstructions of the main fat pathways (posterior dorsal bursae, blue; anterior dorsal bursae, red; melon and the branches of the melon, yellow) and the skull of *Pontoporia blainvillei* (A, B), *Phocoena phocoena* (C, D) and *Tursiops* spp. (E, F) in lateral view.

Changes in the relative size of the rostrum occurred early in development in *Phocoena phocoena* and *L. albirostris* compared to *Pontoporia blainvillei*, thus representing a post-displacement process reducing the size of the rostrum at foetal stages or a pre-displacement process in the Pontoporiidae line. All perinatal and postnatal ontogenies studied here showed an increased size of the rostrum, thus representing a distinct, shared process of the three groups analysed. Interestingly, some small dolphins such as *Delphinus* exhibit an increased rostrum size, representing an undefined peramorphic process.

In odontocetes except Physeteroidea, the branches of the melon might have be useful for collimating sounds in all delphinidan families. The left branch of the melon presented great variation among delphinidans. Particularly in Delphinidae, this character exhibited two reversions (Fig. 9). The absence of the left fat pathway is intrinsically related to the accelerated process of left nasal plug muscle development (Figs 4, 8). In this way, delphinids exhibiting this structure such as *Grampus griseus* evolved under a neotenic process (especially in postnatal development) in the formation of the left side of the epicranial complex. Delphinids also exhibited a distinct configuration distinct from all odontocetes except Physeteroidea, in which the bursae complex is not aligned with the posterior portion of the melon (Character 325, state = 1). As dorsalwards extensions of both posterior premaxillary bone surfaces were observed in the postnatal development of *Pontoporia blainvillei* and *Phocoena phocoena*, it would be plausible to assume that delphinids, lacking this extension, have been subject to a progenetic process in the formation of the posterior portion of the premaxillary and maxillary bones, resulting in a distinct arrangement of the soft tissues (Figs 6, 7, 9). Additionally, delphinids exhibited a distinct arrangement of the nasal diverticula: the premaxillary air sacs became larger than the vestibular air sacs (Character 328, state = 1). In this case, independent processes might have been involved in the size regulation of each structure, such as a progenetic process in the development of the vestibular air sacs in delphinids (i.e. during perinatal and postnatal development), followed by a hypermorphic process in the premaxillary air sacs.

DISCUSSION

Cetacean bauplan evolution is linked to the adaptations of these top predators to subsist throughout all life phases in the aquatic environment. The transition from terrestrial to aquatic organisms has led to a large number of developmental-based changes of individual organ systems (Thewissen & Williams, 2002; Berta *et al.*, 2014). Besides evolutionary novelties related to hydrodynamic locomotion and propulsion (Fish, 2002; Thewissen *et al.*, 2009), stem cetaceans from the Eocene (56–33.9 Mya) evolved unique arrangements of the sound-receiving structures due to adaptation for directional underwater hearing (Oelschläger, 1990; Nummela *et al.*, 2004). A gradual shift of the external naris to the top of the head occurred in concert with the so-called 'telescoping' process of the cetacean skull (Miller, 1923). Accordingly, the rostrum increased in size and in the number of specialized teeth to catch and grab small invertebrates and fishes (Armfield *et al.*, 2013). The posterior portion of the upper jaw bones (maxillary and premaxillary bones) extended caudally and resulted in rearrangement of the forehead muscles and soft tissues to open and occlude the nasal passage during diving behaviours (Heyning

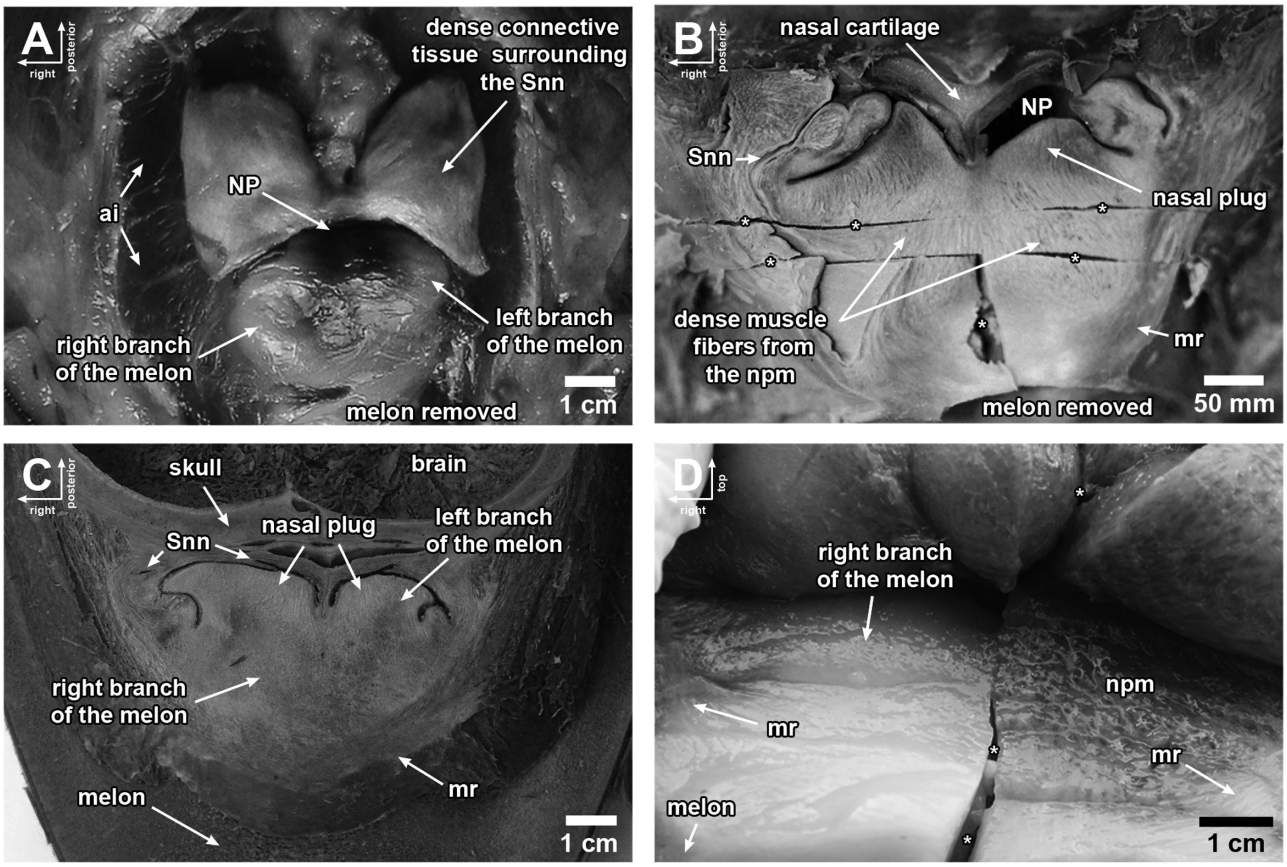

Figure 8. Dorsal photographs of dissections (horizontal cuts) of epicranial complexes in *Pontoporia blainvillei* (A), *Phocoena phocoena* (B), neonatal *Tursiops truncatus* (C) and an adult *Tursiops gephyreus* (D) showing interspecific variation in the main structures involved in sound modulation. Abbreviations: ai, Musculus maxillonasolabialis anterointernus; mr, Musculus maxillonasolabialis rostralis; NP, nasal passage; npm, nasal plug muscle; Snn, Saccus nasalis nasofrontalis. Asterisks indicate artefacts due to mechanical impacts during dissection.

& Mead, 1990; Geisler *et al.*, 2014). Major changes occur during morphogenesis of the cetacean skull (Kükenthal, 1889; Klima, 1999; Moran *et al.*, 2011) and are promoted primarily by the unique transformation of the nasal cartilages in foetal stages (Fig. 1) (Klima, 1999). In odontocetes, the transformations during foetal development of the nasal cartilage affect the soft nasal tissue morphology found in adults. Although many studies have attempted to analyse the prenatal development and evolution of the cetacean skeleton (Moran *et al.*, 2011), few studies have addressed the ontogeny of the soft tissues and its macroevolutionary implications (Klima, 1999).

Extant cetaceans, i.e. baleen (suborder Mysticeti) and toothed (suborder Odontoceti) whales, show similar patterns of rostrum formation: the rostrum nasi cartilage starts developing rostralwards during embryogenesis and is retained in all adult forms between the vomer, premaxilla and maxilla as the mesorostral cartilage (Klima, 1999). However, the two lineages differ in the development of individual parts of the nasal cartilage. Mysticetes retain the medial and caudal portion of the nasal cartilage in adults to sustain the inner margin of the blowhole (Buono *et al.*, 2015) while odontocetes present variable ontogenetic trajectories through which the posterior side wall structures are retained in adults (e.g. the left tectum nasi as the unilateral nasal roof cartilage in sperm whales), or are lost during postnatal development (e.g. bursae cartilage in some odontocetes) (Klima, 1995; Prahl *et al.*, 2009). In addition, the skull formation differs between the two suborders mainly due to changes in the development of the skull (Moran *et al.*, 2011): Oelschläger (1990) proposed that the increased rostrum size in early odontocetes resulted in dorsal anchoring of the premaxillary and maxillary bones to the frontal bone (i.e. instead of below the frontal bone in mysticetes). This in turn promoted the development of associated musculature and soft tissues surrounding the nasal passage capable of

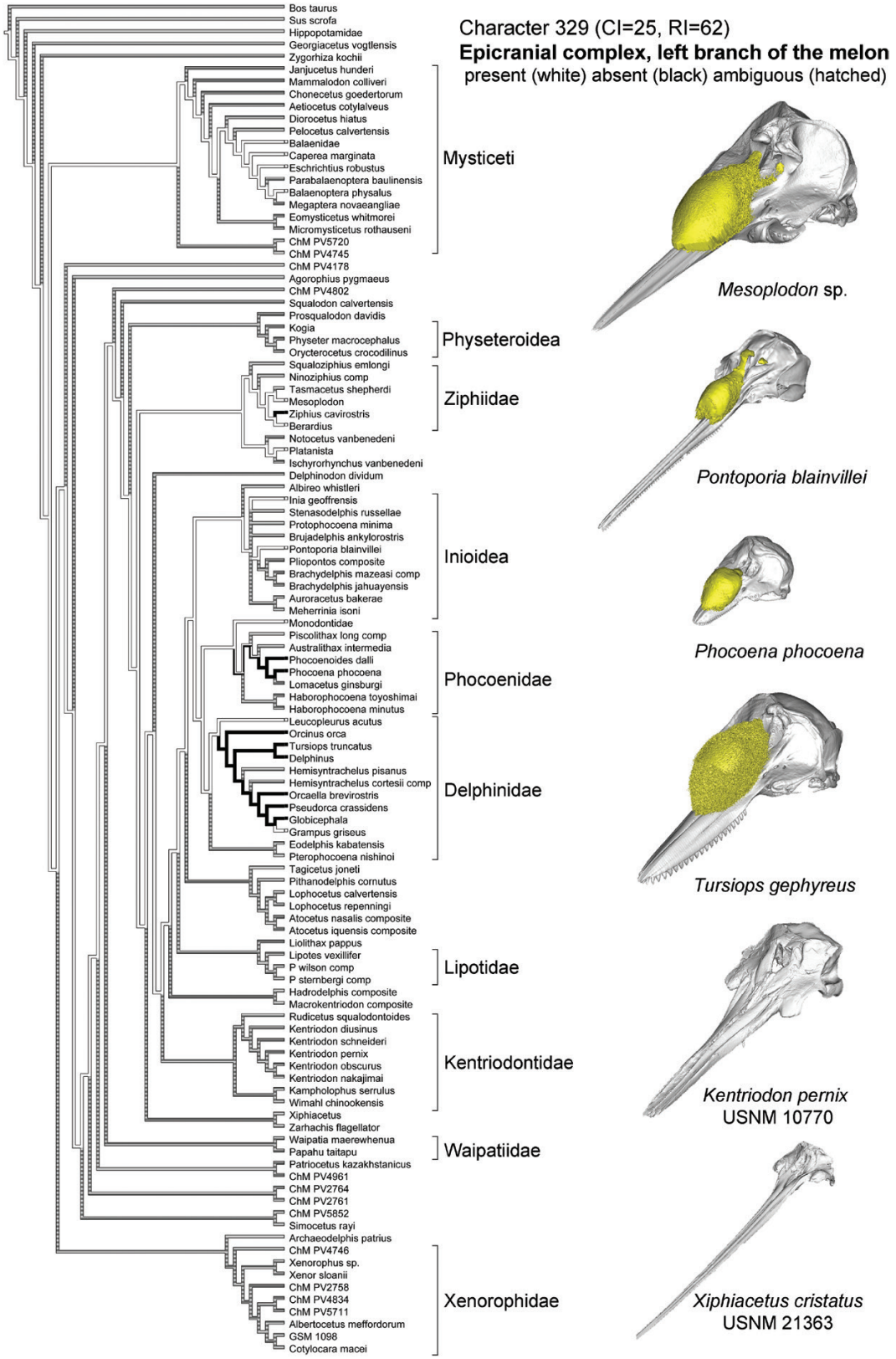

Figure 9. Ancestral character reconstruction using the parsimony method to infer the evolution of the posterior portion of the melon in odontocetes. Character 329 – Epicranial complex, left branch of the melon: present (white), absent (black),

producing and transmitting sounds (Norris *et al.*, 1961; Cranford *et al.*, 1996).

In this study, we demonstrated that ontogenetically based transformations, as proposed in the Extended Evolutionary Synthesis (EES) (Laland *et al.*, 2015), were responsible for the morphological variation in the cetacean head, especially in odontocetes (Fig. 9; Supporting Information, File S1). Body bauplan changes of Carnegie stages C16 to C19 combined with the development of the nasal cartilage may underlie the dorsoposterior movements of the external nasal passage to the vertex of the head (Fig. 1). Although Miller (1923) wrongly named a process (i.e. telescoping) (Churchill *et al.*, 2018) by comparing matured skulls of independently evolved lineages, the transformation described by the author was, in part, perceived in the morphogenesis of the skull (Moran *et al.*, 2011). Thus, the term will be used here to designate this ontogenetically based transformation: the telescoping could be interpreted as a developmental process expressed in distinct transformational patterns among all cetaceans due to variable timing of the formation of nasal cartilages in early foetal life.

Morphological variation of the relative size of the nasal cartilage at early foetal stages might indicate accelerated ontogenetic timing in the formation of the rostrum nasi cartilage at early Carnegie stages in *Pontoporia blainvillei*, compared to *Phocoena phocoena* and *L. albirostris* (Fig. 3). This seems to address the increased rostrum (i.e. premaxillary and maxillary bones) size relative to the epicranial complex in adults (i.e. character 330, state = 0) (Figs 6, 7, 9). As perceived in the ancestral character reconstruction analysis (Supporting Information, File S1), an increased rostrum size relative to the ECL (see Material and Methods) seems to represent a plesiomorphic condition in odontocetes, after which two main convergent paedomorphic events have occurred (i.e. family Ziphiidae and Delphinoidea clade) with, at least, one reversion within each clade (i.e. *Ziphius cavirostris* and *D. delphis*, respectively; Supporting Information, File S1). Thus, the small size of the rostrum nasi in *Phocoena phocoena* and *L. albirostris*, compared to *Pontoporia blainvillei*, might represent variable expression of regulatory mechanisms during early formation of the nasal cartilage in these groups (Figs 1, 3) as observed in other parts of the body such as hind-limb development (Thewissen *et al.*, 2006). The fact that the ossification in our *Phocoena* foetuses was earlier at the nasal complex than in the ear (tympanoperiotic complex) seems to contradict the hypothesis that the head structures involved in echolocation develop ontogenetically in the same order as they appeared during evolution of toothed whales (Haddad *et al.*, 2012). However, the shape and configuration of the soft nasal structures develop later in early *Phocoena* foetuses than the ear structures.

The presence of a pair of bursae cartilages (bc) found just posterior of each posterior dorsal bursa in dolphins (Cranford *et al.*, 1996) and neonatal *Phocoena phocoena* (Prahl *et al.*, 2009) were crucial to topographically determine the precursor tissues as posteriorly positioned relative to the nasal passage (Fig. 2F). Heyning (1989) also described a thin cartilage in the blowhole ligament (posterior to the nasal passage) of *Delphinapterus leucas*. All specimens analysed in this study, including *M. monoceros* analysed by Comtesse-Weidner (2007), presented this flatted cylinder of cartilage in parallel to the nasal passage associated with a loose connective tissue composed of mesenchymal cells at foetal stages (Figs 2–4A", B", C"). Comtesse-Weidner (2007) proposed that the entire loose connective tissue from TA1 may represent the precursor tissue of the bursae complex (i.e. posterior dorsal bursae). However, we suggest that the mentioned tissue together with the concentric collagen and muscle fibres, the intrinsic muscle (Heyning, 1989) (Figs 2–4), may differentiate into the connective tissue surrounding the posterior nasofrontal air sacs (Fig. 2C). This is plausible because the precursor tissue of the posterior dorsal bursae seems to be restricted to the loose connective tissue between the bursae cartilage, posteriorly, and the nasal passage (Fig. 2F). Therefore, we assume that similar mesenchymal loose connective tissue (e.g. TA1) might originate fat (i.e. precursor tissue), soft or dense connective tissues.

Independently acquired features – i.e. homoplasies or repeated evolution – in isolated lineages may be due to convergent selection and/or developmental bias (Laland *et al.*, 2015). In this way, it would be plausible that the concentric and dense connective tissues surrounding the nasal diverticula in *Kogia*, the 'vocal cap' (Thornton *et al.*, 2015), might represent a distinct ontogenetic derivation of the early loose connective tissue. This is composed of likewise concentrically arranged collagen and muscle fibres (i.e. posterior loose connective tissue in TA1) at early foetal stages in *Phocoena*, *Pontoporia*, *Lagenorhynchus* (Figs 2–4) and *Monodon* (Comtesse-Weidner, 2007). Interestingly, the posterior nasofrontal air sacs in *Globicephala*, *Orcaella* and *Pontoporia* (Mead, 1975; Arnold & Heinsohn, 1996; Frainer *et al.*, 2015) and the

ambiguous (hatched). All 3D models containing the main fat pathways (yellow) in the epicranial complex were provided in this study (see Material and Methods), while the remaining models were taken from Phenome10k library (http://phenome10k.org/). Classification follows Lambert *et al.* (2017).

'vocal cap' in *Kogia* (Thornton *et al.*, 2015) exhibit a similar trabecular structure associated with the dense connective tissue. However, further studies should address the topic in detail and investigate the early soft nasal tissues in *Physeter* and *Kogia*. Distinct trajectories of this connective tissue ontogeny might represent one among other adaptations for NBHF sound production (Madsen *et al.*, 2005; Kyhn *et al.*, 2010) (see below) as the connective tissue surrounding the posterior portion of the nasofrontal air sacs is highly anatomically specialized in *Pontoporia blainvillei* and *Phocoena phocoena* – i.e. the porpoise capsule (see Cranford *et al.*, 1996; Huggenberger *et al.*, 2009) – and presumably developed to a lesser degree in broadband species, such as *Globicephala* (Mead, 1975) and *Orcaella* (Arnold & Heinsohn, 1996).

The soft nasal tissues positioned just anterior to the nasal passage (i.e. TA3) at early foetal stages (Fig. 1) presented similar differentiation as TA1: the loose appearing connective tissue composed of cells with large intercellular spaces surrounding the septum nasi cartilage is the origin of the fat and dense connective tissues in adults (Heyning, 1989) (Fig. 8). In most odontocetes, the right branch of the melon is mostly filled by fat and connects the right MLDB complex to the main body of the melon (Cranford *et al.*, 1996; Harper *et al.*, 2008; McKenna *et al.*, 2012). The shape and existence of the melon's left branch is notably variable among species (Fig. 9). The left branch is developed and observed to be connecting its dorsocaudal portion to the left anterior dorsal bursa in *Pontoporia blainvillei*, *Stenella longirostris*, *Sousa plumbea*, *G. griseus* and *Lagenorhynchus obliquidens* (Cranford, 1988; Cranford *et al.*, 1996; McKenna *et al.*, 2012; Frainer *et al.*, 2015, 2019). In some species, the left branch of the melon is almost occluded by a dense connective tissue and muscle fibres from the nasal plug muscles, such as in *Tursiops* (Cranford *et al.*, 1996; Harper *et al.*, 2008) and *Phocoena phocoena* (Huggenberger *et al.*, 2009; Prahl *et al.*, 2009) (Fig. 8). Interestingly, a pair of fat bodies embedded within the nasal plug muscles is described in some baleen whales (Heyning & Mead, 1990; Buono *et al.*, 2015) to presumably '… allow the free movement of the nasal plugs as they are retracted by the nasal plug muscles during respiration …' (Heyning & Mead, 1990). Heyning & Mead (1990) pointed out that the pair of fat bodies embedded within the nasal plug muscles are presumably homologous to the melon of odontocetes. If this is the case, this structure originated in a common ancestor of both extant lineages (see below).

Cephalic adipose tissues in the human face are known to be derived from neural crest cells (Billon & Dani, 2012), which presumably give rise to chondrocytes and possibly other mesenchymal cells (Billon *et al.*, 2007). Accordingly, the adipose tissue depots in the human head constitute distinct small organs exhibiting functional differences and variable contribution to metabolic dysfunctions, such as obesity (Billon & Dani, 2012). Although the cellular and molecular mechanisms responsible for the formation of the fat tissues in the mammalian face remain unclear, we have demonstrated that the evolution of odontocetes was remarkable in the great variation in the site-specific ontogenetic regulation of the cephalic adipose tissues (Billon & Dani, 2012). The morphological variation in the composition of the 'posterior melon' (Harper *et al.*, 2008) (Fig. 9) may address specific adaptations to sound production among non-physeteroid odontocetes (Frainer *et al.*, 2019). Most non-physeteroid odontocetes exhibit the right branch of the melon connected to its main body (character 327, state = 0) (Figs 5, 8D, 9), except for *Globicephala*, *Cephalorhynchus* (Mead, 1975) and *Lagenorhynchus obliquidens* (Cranford *et al.*, 1996). In these species, the two structures are separated by dense connective tissue (character 327, state = 1), which seems to represent hypertrophied Musculus maxillonasolabialis rostralis (mr) tendons and associated dense connective tissue derived from TA2 in foetal development (Comtesse-Weidner, 2007) (Figs 1, 4). In this study, we demonstrated that the branches of the melon, or the posterior melon (*sensu* Harper *et al.*, 2008), and the melon actually represent distinct structures derived from independent primordial tissues, under presumably distinct regulatory factors according to the morphological variation found in odontocetes (Fig. 9). In this respect, we propose two new designations for both right and left branches of the melon to address homology comparisons: Corpus adiposum nasalis terminalis pars posterioris dexter (Cand) and Corpus adiposum nasalis terminalis pars posterioris sinister (Cans), respectively.

Ontogenetically, the melon originates later than the nasal plug muscles and associated connective tissues given that muscle fibres from the Musculus maxillonasolabialis rostralis (mr) start developing into TA4 in late foetal stages (Carnegie stages F18 and F19) concomitant with increased differentiation of the blubber precursor tissues (Fig. 1). Increased fat production between mr layers start late in foetal stages and continue through the perinatal (Fig. 5) and postnatal development to form the melon (Figs 6, 7, 9). The distinction between different main fat bodies positioned anterior to the nasal passage in odontocetes gave rise to distinct cladistic interpretations for the origin of the melon in Cetacea (Heyning, 1989), which is exclusive (autapomorphic) for odontocetes (Supporting Information, File S1) and may be correlated to the acquisition of ultrasound hearing in cetaceans (Churchill *et al.*, 2016; Galatius *et al.*, 2018).

The existence and shape differences of the branches of the melon (i.e. Cand and Cans) presented great morphological variation into Delphinoidea: the Cand was commonly present in most non-physeteroid odontocetes except in phocoenids (Fig. 8B) (Huggenberger *et al.*, 2009; Prahl *et al.*, 2009) while the Cans exhibited variation within Delphinoidea (Fig. 8), and within the family Ziphiidae (Fig. 9). In some lineages (cited above), the left nasal plug muscle exhibits a smaller degree of development compared with dense muscle and collagen fibres, thus allowing the primordial loose connective tissue from TA3 to give rise to Cans just below the anterior dorsal bursae (character 309, state = 0). However, in phocoenids, most delphinids (Fig. 8) and *Ziphius cavirostris* (Heyning, 1989), the left-hand side nasal plug muscle was hypertrophied and completely replaced the pathway between the bursae complex (i.e. precursor tissue and anterior dorsal bursae) and the melon (character 329, state = 1) (Fig. 9). The postnatal development of the left nasal plug muscle and the replacement of the Cans in *Tursiops* may polarize this ontogenetic-based transformation, as it seems to represent paedomorphic events in delphinids that exhibit such a structure.

The development of the nasal air sacs revealed a distinct timing of formation, as they develop independently in a sequence of steps: first premaxillary air sacs and nasofrontal air sacs, and then the vestibular air sacs. Interestingly, the presence of premaxillary air sacs may represent a conserved condition in non-physeteroid odontocetes (Schenkkan, 1973; Mead, 1975; Heyning, 1989). The vestibular air sacs seem to represent the most variable nasal air sac in dolphin-sized species. In *Lipotes vexillifer* (Chen *et al.*, 1980), *Inia geoffrensis* (Schenkkan, 1973), *Pontoporia blainvillei* (Frainer *et al.*, 2015) and *Phocoena phocoena* (Huggenberger *et al.*, 2009), this structure has larger dimensions than the premaxillary air sacs (character 328, state = 0). In delphinids, by contrast, the reverse size relationship (premaxillary air sacs > vestibular air sacs) in the nasal diverticula (character 328, state = 1) might represent distinct adaptations for sound production (see below). Ancestral character reconstruction analysis represented a cladistic method to presume the soft nasal morphology of extinct odontocetes and to map major changes linked to the evolution of the sound production and modulation structures in these complex echolocating and social mammals (Supporting Information, File S1).

Echolocation and communication signals have evolved under the concomitant constraints of body size (Au, 1993), social (May-Collado *et al.*, 2007) and biosonar properties (Jensen *et al.*, 2018). The directional properties of a sound emission apparatus tend to increase the source level (dB) in the forward direction where click energy exhibits elevated center frequency (kHz) and increasing target detection range (Jensen *et al.*, 2009; Koblitz *et al.*, 2012; Finneran *et al.*, 2014). In the dolphin head, the sound beam interacts with the skull, dense connective tissue theca (character 326, state = 0) and the vestibular air sacs (Wei *et al.* 2017). It is collimated through the Cand (i.e. for navigation and hunting) or Cans (i.e. for communication) (Madsen *et al.*, 2013) – or simultaneously (Ridgway *et al.*, 2015) – to the melon (Wei *et al.*, 2017). Since fat pathways are important for absorbing and collimating shorter wavelengths (i.e. high frequency) (Amundin & Andersen, 1983), the morphological variability in the composition of the nasal plug muscle might represent adaptations for high-frequency communication in some dolphin-sized odontocetes such as *Stenella longirostris*, *G. griseus*, *L. albirostris*, *Pontoporia blainvillei* and *Sousa plumbea* (Frainer *et al.*, 2019). The melon collimates the sound and effectively transmits it into the aquatic environment by impedance matching (Harper *et al.*, 2008; McKenna *et al.*, 2012).

The general morphology of the sound-generating structures in extant NBHF species revealed a distinct topographical arrangement (Table 2). However, presumably homoplasic conditions promoted by distinct ontogenetic trajectories may represent an adapted biosonar apparatus for the production of highly directional sounds: *Kogia* species exhibit short rostra and a dense chamber of connective tissue in the right nasal passage involved in sound production (Thornton *et al.*, 2015). As cited above, the dense connective tissue surrounding the nasofrontal air sacs in *Pontoporia blainvillei* and *Phocoena phocoena* might address adaptation for high-frequency sound production (Huggenberger *et al.*, 2009). Interestingly, the horizontal alignment of the bursae complex with the posterior portion of the melon (Fig. 7) (character 325, state = 0) was perceived in *Phocoena phocoena*, *Pontoporia blainvillei* and *Cephalorhynchus commersonii* and might represent a plesiomorphic character in Delphinida since it was observed in *Mesoplodon* and *Platanista gangetica* (not shown in figures). Galatius & Goodall (2016) reported a comparatively less concave profile in the skulls of *Lagenorhynchus australis* and *Cephalorhynchus* dolphins, which might signify NBHF properties. On the other hand, the authors demonstrated that *Lagenorhynchus cruciger*, which also produces NBHF clicks, presented a more concave skull profile compared to the other species. Thus, it might represent adaptations for modulating the sound beam, or, alternatively, may be related to the production of derived communication sounds, as *Lagenorhynchus cruciger* shows increased social complexity compared to its closest relatives (Galatius *et al.*, 2018).

Table 2. Comparative anatomy of the main structures involved in sound modulation in the dolphin head

Species	Rostrum size	Relative volume of the nasal diverticula	Branches of the melon	Connective tissue theca	Fat pad topography	Directional properties of the sound source
Pontoporia blainvillei	Long and narrow	Vestibular air sacs > premaxillary air sacs	Both present	Covering both lateral walls of the epicranial complex	The bursae complex is aligned horizontally to the melon's branches	Narrow-band high-frequency sounds
Inia geoffrensis	Long and narrow	Vestibular air sacs > premaxillary air sacs	Both present	Covering both lateral walls of the epicranial complex	The bursae complex is aligned horizontally to the melon's branches	Broad-band low- and high-frequency sounds with highly directional properties*
Phocoena phocoena	Short	Vestibular air sacs > premaxillary air sacs	Both absent	Covering both lateral walls of the epicranial complex	The bursae complex is aligned horizontally to the melon's branches	Narrow-band high-frequency sounds
Tursiops sp.	Short	Vestibular air sacs < premaxillary air sacs	Right present and left absent	Covering only the dorsal portion of the epicranial complex	The bursa complex is dorsoposteriorly positioned relative to the melon's branches	Broad-band sounds in lower frequency
Cephalorhynchus sp.	Short	Vestibular air sacs > premaxillary air sacs	Right present and left absent	Covering both lateral walls of the epicranial complex	The bursae complex is aligned horizontally to the melon's branches	Narrow-band high-frequency sounds

*See Ladegaard *et al.* (2015).

The morphology of the nasal tract in odontocetes evolved under several heterochronic processes linked to the development of main structures involved in sound beam modulation (Fig. 9; Supporting Information, File S1). Paedomorphic events related to decreasing rostrum size in adults may have occurred at least three times in odontocete evolution (i.e. Kogiidae, Ziphiidae and Delphinoidea clade), together with presumable changes in the directionality of the sound emitted. The increased rostrum length might represent an important component influencing sound modulation in some groups such as *Pontoporia blainvillei* and *Lipotes vexillifer* (Wei *et al.*, 2017; Frainer *et al.*, 2019). We did not consider rostrum size reduction in *Physeter macrocephalus* because, in this species, the soft nasal tissue is hypertrophied due to specializations for highly directional, high-energy sounds (Møhl *et al.*, 2000). Most members of Delphinidae and Monodontidae are broad-band echolocators (Galatius *et al.*, 2018; Jensen *et al.*, 2018) with derived low-frequency modulated sounds for communication (i.e. whistles) besides pulsed calls (i.e. clicks for communication or burst clicks) (May-Collado *et al.*, 2007).

Morphological adaptations of Delphinoidea found in this study seem to have contributed to changes in the directional properties of the sound emission apparatus in comparison to other odontocetes. These morphological characters are: (1) the inverse size relationship of the nasal diverticula (character 328, state = 1) (Supporting Information, File S1); (2) the off-axis alignment of the dorsal bursae with the posterior portion of the melon (character 325, state = 1, also observed in *Z. cavirostris*) (File S1) (Frainer *et al.*, 2019); (3) the development of muscle and dense collagen fibres in the nasal plug muscle with the loss of fat pathways (e.g. Cans) for a distinct timbre of lower frequencies in most delphinids (Frainer *et al.*, 2019); and (4) the decreased rostrum size (Wei *et al.*, 2014). Although in *Phocoena phocoena* both nasal plug muscles are composed of muscle and collagen fibres, the arrangements of other structures are likely to be adaptations for the highly directional sonar, such as large vestibular air sacs, dense connective tissue surrounding the epicranial complex, and the alignment of the sound source with the posterior portion of the melon (Fig. 9; File S1). Topographical changes in the main fat pathways in *Pontoporia blainvillei* and *Phocoena phocoena* (Fig. 7) are promoted by dorsal movements of the posterior portion of the premaxillary bone during postnatal development, thus elevating the premaxillary air sacs and, consequently, the nasal plug muscle and anterior dorsal bursae tissues dorsally. In this way, the ancestral character reconstruction analysis provided cues to determine not only the soft nasal tissues of extinct organisms but also their presumable function.

Kentriodontids (family Kentriodontidae) were small (approximately 2 m long) dolphin-like odontocetes living in neritic and shelf zones of the Pacific and Atlantic oceans, with a pan-tropical to temperate distribution (Barnes, 1978; Ichishima *et al.*, 1994). The decline of kentriodontods was associated with changes in oceanic temperatures and the rising of recent lineages, such as delphinids, in the late Miocene (Ichishima *et al.*, 1994). Among this large group of echolocating fish-predators were the common ancestors of all known dolphins (Lambert *et al.*, 2017; Peredo *et al.*, 2018), and thus functional interpretations based on kentriodontid morphology may elucidate the plesiomorphic condition of the sound emission apparatus. Galatius *et al.* (2018) found that *Kentriodon pernix* (Fig. 9) exhibited an inner ear morphology similar to extant NBHF species, and, thus, it is plausible to assume such capabilities for this extinct dolphin. The sound emission apparatus of *K. pernix* developed under a symmetric skull condition (Barnes, 1978) as in *Pontoporia blainvillei* and *Phocoena phocoena* (Fig. 9), and with less concavity than in *C. commersonii*. By interpreting the ancestral character reconstruction analysis, the presumably soft nasal tissue morphology of *K. pernix* was surrounded by a dense connective tissue and was composed of larger vestibular air sacs compared to the premaxillary air sacs (character 328, state = 0); both Cand and Cans developed (character 329, state = 0); bursae complexes, aligned (character 325, state = 0) with the posterior portion of the melon; and a long rostrum compared to the size of the melon (character 330, state = 0). Thus, the phylogenetic mapping of distinct structures involved in sound production (Supporting Information, File S1) suggests that kentriodontids might have exhibited unique soft nasal tissue morphology adapted for highly directional sounds, as previously proposed (Galatius *et al.*, 2018) and corroborates our hypothesis that extant broadband vocalizing delphinids have evolved under more relaxed constraints regarding directionality of the sonar beam.

In this study, a cladistic mapping of the evolution of the main structures of the sound generation structures in dolphins was performed and interpreted in the light of the EES. The EES assumes that developmental (ontogenetic) mechanisms, operating through developmental bias (e.g. telescoping process in cetaceans) and inclusive inheritance (e.g. cultural transmission for echolocation and communication in toothed whales) along with natural selection (Darwin, 1859), share responsibility for the direction and rate of evolution, thus contributing to organism–environment complementarity (Laland *et al.*, 2015). Following the ancestral character reconstruction analysis, it is reasonable to propose that extant coastal NBHF species represent highly specialized sound generation and emission systems which evolved at least four times

independently of each other under distinct ontogenetic regulations of the formation of the main structures involved in the modulation of echolocation as well as communication sounds.

ACKNOWLEDGEMENTS

G.F. was supported by a PhD scholarship from Coordenação de Aperfeiçoamento de Pessoal de Nível Superior (CAPES) (from 2015 to 2019) and Conselho Nacional de Desenvolvimento Científico e Tecnológico (CNPq) (Ciências Sem Fronteiras – grant number 201709/2015-5). N.S. was supported by a master's scholarship from CNPq (grant number 130940/2017-8). We are grateful to Marc Tittgemeyer from the Max-Planck Institute for Metabolism Research for his assistance with the MRI scans, and to Tiago P. de Carvalho and Luiz R. Malabarba for their comments and suggestions that helped to improve this study. We thank two anonymous reviewers for their helpful comments. A special thanks to all members of the Laboratório de Sistemática e Ecologia de Aves e Mamíferos Marinhos (LABSMAR/UFRGS) and the Department II of Anatomy (University of Cologne). This is a contribution of the Research Group 'Evolução e Biodiversidade de Cetáceos/CNPq'.

REFERENCES

Alberch P, **Gould SJ**, **Oster GF**, **Wake DB. 1979.** Size and shape in ontogeny and phylogeny. *Paleobiology* **5:** 296–317.

Amundin M, **Andersen SH. 1983.** Bony nares air pressure and nasal plug muscle activity during click production in the harbour porpoise, *Phocoena phocoena*, and the bottlenosed dolphin, *Tursiops truncatus*. *Journal of Experimental Biology* **105:** 275.

Armfield BA, **Zheng Z**, **Bajpai S**, **Vinyard CJ**, **Thewissen J. 2013.** Development and evolution of the unique cetacean dentition. *PeerJ* **1:** e24.

Arnold PW, **Heinsohn GE. 1996.** Phylogenetic status of the Irrawaddy dolphin *Orcaella brevirostris* (Owen in Gray): a cladistic analysis. *Memoirs of the Queensland Museum* **39:** 141–204.

Aroyan JL, **Cranford TW**, **Kent J**, **Norris KS. 1992.** Computer modeling of acoustic beam formation in *Delphinus delphis*. *The Journal of the Acoustical Society of America* **92:** 2539–2545.

Au WL. 2000. Hearing in whales and dolphins: an overview. In: Au WL, Richard RF, eds. *Hearing by whales and dolphins.* New York: Springer, 1–42.

Au WW, **Houser DS**, **Finneran JJ**, **Lee WJ**, **Talmadge LA**, **Moore PW. 2010.** The acoustic field on the forehead of echolocating Atlantic bottlenose dolphins (*Tursiops truncatus*). *The Journal of the Acoustical Society of America* **128:** 1426–1434.

Au WWL. 1993. *The sonar of dolphins.* New York: Springer.

Barnes LG. 1978. A review of *Lophocetus* and *Liolithax* and their relationships to the delphinoid family Kentriodontidae (Cetacea: Odontoceti). *Natural History Museum of Los Angeles County Science Bulletin* **28:** 1–35.

Berta A, **Ekdale EG**, **Cranford TW. 2014.** Review of the cetacean nose: form, function, and evolution. *The Anatomical Record* **297:** 2205–2215.

Billon N, **Dani C. 2012.** Developmental origins of the adipocyte lineage: new insights from genetics and genomics studies. *Stem Cell Reviews and Reports* **8:** 55–66.

Billon N, **Iannarelli P**, **Monteiro MC**, **Glavieux-Pardanaud C**, **Richardson WD**, **Kessaris N**, **Dani C**, **Dupin E. 2007.** The generation of adipocytes by the neural crest. *Development* **134:** 2283–2292.

Buono MR, **Fernández MS**, **Fordyce RE**, **Reidenberg JS. 2015.** Anatomy of nasal complex in the southern right whale, *Eubalaena australis* (Cetacea, Mysticeti). *Journal of Anatomy* **226:** 81–92.

Chen P, **Lin K**, **Liu R**. **1980.** Study of the anatomy and histology of the upper respiratory tract of *Lipotes vexillifer* Miller. *Acta Hydrobiologica Sinica* **2:** 131–137 [in Chinese, English abstract].

Churchill M, **Geisler JH**, **Beatty BL**, **Goswami A. 2018.** Evolution of cranial telescoping in echolocating whales (Cetacea: Odontoceti). *Evolution* **72:** 1092–1108.

Churchill M, **Martinez-Caceres M**, **de Muizon C**, **Mnieckowski J**, **Geisler JH. 2016.** The origin of high-frequency hearing in whales. *Current Biology: CB* **26:** 2144–2149.

Comtesse-Weidner P. **2007.** *Untersuchungen am Kopf des fetalen Narwals Monodon monoceros: Ein Atlas zur Entwicklung und funktionellen Morphologie des Sonarapparates*. Giessen: VVB Laufersweiler Verlag.

Cranford TW. 1988. The anatomy of acoustic structures in the spinner dolphin forehead as shown by x-ray computed tomography and computer graphics. In: Nachtigall PE, Moore PWB, eds. *Animal sonar: processes and performance.* Boston: Springer, 67–77.

Cranford TW, **Amundin M**, **Norris KS. 1996.** Functional morphology and homology in the odontocete nasal complex: implications for sound generation. *Journal of Morphology* **228:** 223–285.

Cranford TW, **McKenna MF**, **Soldevilla MS**, **Wiggins SM**, **Goldbogen JA**, **Shadwick RE**, **Krysl P**, **St Leger JA**, **Hildebrand JA. 2008.** Anatomic geometry of sound transmission and reception in Cuvier's beaked whale (*Ziphius cavirostris*). *The Anatomical Record* **291:** 353–378.

Darwin C. **1859.** *On the origin of the species.* London: Routledge.

De Queiroz K. **1985.** The ontogenetic method for determining character polarity and its relevance to phylogenetic systematics. *Systematic Zoology* **34:** 280–299.

Fink WL. 1982. The conceptual relationship between ontogeny and phylogeny. *Paleobiology* **8:** 254–264.

Finneran JJ, **Branstetter BK**, **Houser DS**, **Moore PW**, **Mulsow J**, **Martin C**, **Perisho S. 2014.** High-resolution measurement of a bottlenose dolphin's (*Tursiops truncatus*) biosonar transmission beam pattern in the horizontal plane. *The Journal of the Acoustical Society of America* **136:** 2025–2038.

Fish FE. 2002. Balancing requirements for stability and maneuverability in cetaceans. *Integrative and Comparative Biology* **42:** 85–93.

Fox KCR, **Muthukrishna M**, **Shultz S. 2017.** The social and cultural roots of whale and dolphin brains. *Nature Ecology & Evolution* **1:** 1699–1705.

Frainer G, **Huggenberger S**, **Moreno IB. 2015.** Postnatal development of Franciscana's (*Pontoporia blainvillei*) biosonar relevant structures with potential implications for function, life history, and bycatch. *Marine Mammal Science* **31:** 1193–1212.

Frainer G, **Plön S**, **Serpa NB**, **Moreno IB**, **Huggenberger S**. **2019.** Sound generating structures of the humpback dolphin *Sousa plumbea* (cuvier, 1829) and the directionality in dolphin sounds. *The Anatomical Record* **302:** 849–860.

Galatius A, **Goodall RN. 2016.** Skull shapes of the Lissodelphininae: radiation, adaptation and asymmetry. *Journal of Morphology* **277:** 776–785.

Galatius A, **Olsen MT**, **Steeman ME**, **Racicot RA**, **Bradshaw CD**, **Kyhn LA**, **Miller LA. 2018.** Raising your voice: evolution of narrow-band high-frequency signals in toothed whales (Odontoceti). *Biological Journal of the Linnean Society* **126:** 213–224.

Geisler JH, **Colbert MW**, **Carew JL. 2014.** A new fossil species supports an early origin for toothed whale echolocation. *Nature* **508:** 383–386.

Goloboff PA, **Farris JS**, **Nixon KC. 2008.** TNT, a free program for phylogenetic analysis. *Cladistics* **24:** 774–786.

Gould SJ. 1977. *Ontogeny and phylogeny*. Cambridge: Harvard University Press.

Haddad D, **Huggenberger S**, **Haas-Rioth M**, **Kossatz LS**, **Oelschläger HHA**, **Haase A**. **2012.** Magnetic resonance microscopy of prenatal dolphins (Mammalia, Odontoceti, Delphinidae) – Ontogenetic and phylogenetic implications. *Zoologischer Anzeiger - A Journal of Comparative Zoology* **251:** 115–130.

Harper CJ, **McLellan WA**, **Rommel SA**, **Gay DM**, **Dillaman RM**, **Pabst DA. 2008.** Morphology of the melon and its tendinous connections to the facial muscles in bottlenose dolphins (*Tursiops truncatus*). *Journal of Morphology* **269:** 820–839.

Heyning JE. 1989. Comparative facial anatomy of beaked whales (Ziphiidae) and a systematic revision among the families of extant Odontoceti. *Contributions in Science* **405:** 1–64.

Heyning JE, **Mead JG. 1990.** Evolution of the nasal anatomy of cetaceans. In: Thomas JA, Kastelein RA, eds. *Sensory abilities of cetaceans: laboratory and field evidence*. Boston: Springer, 67–79.

Huggenberger S. **2004.** *Functional morphology, development, and evolution of the upper respiratory tract in toothed whales (Odontoceti)*. Unpublished D. Phil. Thesis, Johann Wolfgang Goethe-Universität.

Huggenberger S. **2008.** The size and complexity of dolphin brains - a paradox? *Journal of the Marine Biological Association of the United Kingdom* **88:** 1103–1108.

Huggenberger S, **André M**, **Oelschläger HHA. 2014.** The nose of the sperm whale: overviews of functional design, structural homologies and evolution. *Journal of the Marine Biological Association of the United Kingdom* **96:** 783–806.

Huggenberger S, **Rauschmann MA**, **Vogl TJ**, **Oelschläger HH. 2009.** Functional morphology of the nasal complex in the harbor porpoise (*Phocoena phocoena* L.). *The Anatomical Record* **292:** 902–920.

Huxley J. **1942.** *Evolution - the modern synthesis*. London: George Allen and Unwin.

Ichishima H, **Barnes LG**, **Fordyce RE**, **Kimura M**, **Bohaska DJ. 1994.** A review of kentriodontine dolphins (Cetacea; Deiphinoidea; Kentriodontidae): systematics and biogeography. *Island Arc* **3:** 486–492.

Jensen FH, **Bejder L**, **Wahlberg M**, **Madsen PT. 2009.** Biosonar adjustments to target range of echolocating bottlenose dolphins (*Tursiops* sp.) in the wild. *The Journal of Experimental Biology* **212:** 1078–1086.

Jensen FH, **Johnson M**, **Ladegaard M**, **Wisniewska DM**, **Madsen PT. 2018.** Narrow acoustic field of view drives frequency scaling in toothed whale biosonar. *Current Biology: CB* **28:** 3878–3885.e3.

Kimura T, **Hasegawa Y**. **2019.** A new species of Kentriodon (Cetacea, Odontoceti, Kentriodontidae) from the Miocene of Japan. *Journal of Vertebrate Paleontology*: e1566739.

Kleinenberg SC, **Yablokov AV. 1958.** The morphology of the upper respiratory tract of whales. *Zoologichesk Zhurnal* **37:** 1091–1099.

Klima M. **1995.** Cetacean phylogeny and systematics based on the morphogenesis of the nasal skull. *Aquatic Mammals* **21:** 79–89.

Klima M. **1999.** *Development of the cetacean nasal skull*. Berlin: Springer.

Klingenberg CP. 1998. Heterochrony and allometry: the analysis of evolutionary change in ontogeny. *Biological Reviews* **73:** 79–123.

Kluge AG. 1985. Ontogeny and phylogenetic systematics. *Cladistics* **1:** 13–27.

Koblitz JC, **Wahlberg M**, **Stilz P**, **Madsen PT**, **Beedholm K**, **Schnitzler HU. 2012.** Asymmetry and dynamics of a narrow sonar beam in an echolocating harbor porpoise. *The Journal of the Acoustical Society of America* **131:** 2315–2324.

Kükenthal W. 1893. *Vergleichend-anatomische und entwickelungsgeschichtliche Untersuchungen an Walthieren*. Denkschriften der Medicinisch-Naturwissenschaftlichen Gesellschaft zu Jena **3**: 1–448.

Kyhn LA, **Jensen FH**, **Beedholm K**, **Tougaard J**, **Hansen M**, **Madsen PT. 2010.** Echolocation in sympatric Peale's dolphins (*Lagenorhynchus australis*) and Commerson's dolphins (*Cephalorhynchus commersonii*) producing narrow-band high-frequency clicks. *The Journal of Experimental Biology* **213:** 1940–1949.

Ladegaard M, **Jensen FH**, **de Freitas M**, **Ferreira da Silva VM**, **Madsen PT. 2015.** Amazon river dolphins (*Inia geoffrensis*) use a high-frequency short-range biosonar. *The Journal of Experimental Biology* **218:** 3091–3101.

Laland KN, **Uller T**, **Feldman MW**, **Sterelny K**, **Müller GB**, **Moczek A**, **Jablonka E**, **Odling-Smee J**. **2015.** The extended evolutionary synthesis: its structure, assumptions and predictions. *Proceedings of the Royal Society B: Biological Sciences* **282:** 20151019.

Lambert O, **Bianucci G**, **Urbina M**, **Geisler JH. 2017.** A new inioid (Cetacea, Odontoceti, Delphinida) from the Miocene of Peru and the origin of modern dolphin and porpoise families. *Zoological Journal of the Linnean Society* **179:** 919–946.

Lindberg DR, **Pyenson ND. 2007.** Things that go bump in the night: evolutionary interactions between cephalopods and cetaceans in the Tertiary. *Lethaia* **40:** 335–343.

Maddison WP, **Maddison DR. 2018.** *Mesquite: a modular system for evolutionary analysis. Version 3.51*. Available at: http://www.mesquiteproject.org.

Madsen PT, **Carder DA**, **Bedholm K**, **Ridgway SH. 2005.** Porpoise clicks from a sperm whale nose—convergent evolution of 130 khz pulses in toothed whale sonars? *Bioacoustics* **15:** 195–206.

Madsen PT, **Lammers M**, **Wisniewska D**, **Beedholm K. 2013.** Nasal sound production in echolocating delphinids (*Tursiops truncatus* and *Pseudorca crassidens*) is dynamic, but unilateral: clicking on the right side and whistling on the left side. *The Journal of Experimental Biology* **216:** 4091–4102.

Marino L, **McShea D**, **Uhen MD. 2004.** The origin and evolution of large brains in toothed whales. *Anatomical Record – Advances in Integrative Anatomy and Evolutionary Biology* **281A:** 1247–1255.

May-Collado LJ, **Agnarsson I**, **Wartzok D. 2007.** Phylogenetic review of tonal sound production in whales in relation to sociality. *BMC Evolutionary Biology* **7:** 136.

McKenna MF, **Cranford TW**, **Berta A**, **Pyenson ND. 2012.** Morphology of the odontocete melon and its implications for acoustic function. *Marine Mammal Science* **28:** 690–713.

Mead JG. 1975. Anatomy of the external nasal passages and facial complex in the Delphinidae (Mammalia: Cetacea). *Smithsonian Contributions to Zoology* **207:** 1–35.

Mead JG, **Fordyce RE. 2009.** The therian skull: a lexicon with emphasis on the odontocetes. *Smithsonian Contributions to Zoology* **627:** 1–249.

Miller GS. 1923. The telescoping of the cetacean skull. *Smithsonian Miscellaneous Collection* **75:** 1–55.

Møhl B, **Wahlberg M**, **Madsen PT**, **Miller LA**, **Surlykke A. 2000.** Sperm whale clicks: directionality and source level revisited. *The Journal of the Acoustical Society of America* **107:** 638–648.

Moran MM, **Nummela S**, **Thewissen JG. 2011.** Development of the skull of the pantropical spotted dolphin (*Stenella attenuata*).*The Anatomical Record* **294:** 1743–1756.

Morisaka T, **Connor RC. 2007.** Predation by killer whales (*Orcinus orca*) and the evolution of whistle loss and narrow-band high frequency clicks in odontocetes. *Journal of Evolutionary Biology* **20:** 1439–1458.

NAV. 2017. *Nomina anatomica veterinaria*, *6th edn*. Hanover: World Association of Veterinary Anatomists.

Norris KS, **Prescott JH**, Asa-**Dorian PV**, **Perkins P**. **1961.** An experimental demonstration of echolocation behavior in the porpoise, *Tursiops truncatus* (Montagu). *The Biological Bulletin* **120:** 163–176.

Nummela S, **Thewissen JG**, **Bajpai S**, **Hussain ST**, **Kumar K. 2004.** Eocene evolution of whale hearing. *Nature* **430:** 776–778.

Oelschläger HA. 1990. Evolutionary morphology and acoustics in the dolphin skull. In: Thomas JA, Kastelein RA, eds. *Sensory abilities of cetaceans: laboratory and field evidence*. Boston: Springer, 137–162.

Oelschläger HH, **Ridgway SH**, **Knauth M. 2010.** Cetacean brain evolution: dwarf sperm whale (*Kogia sima*) and common dolphin (*Delphinus delphis*) – an investigation with high-resolution 3D MRI. *Brain, Behavior and Evolution* **75:** 33–62.

Peredo CM, **Uhen MD**, **Nelson MD. 2018.** A new kentriodontid (Cetacea: Odontoceti) from the early Miocene Astoria formation and a revision of the stem delphinidan family Kentriodontidae. *Journal of Vertebrate Paleontology* **38:** e1411357.

de Pinna MCC. 1991. Concepts and tests of homology in the cladistic paradigm. *Cladistics* **7:** 367–394.

Prahl S, **Huggenberger S**, **Schliemann H. 2009.** Histological and ultrastructural aspects of the nasal complex in the harbour porpoise, *Phocoena phocoena*. *Journal of Morphology* **270:** 1320–1337.

Ridgway S, **Samuelson Dibble D**, **Van Alstyne K**, **Price D. 2015.** On doing two things at once: dolphin brain and nose coordinate sonar clicks, buzzes and emotional squeals with social sounds during fish capture. *The Journal of Experimental Biology* **218:** 3987–3995.

Rodionov VA, **Markov VI. 1992.** Functional anatomy of the nasal system in the bottlenose dolphin. In: Thomas JA, Kastelein RA, Supin AY, eds. *Marine mammal sensory systems.* Boston: Springer, 147–177.

Schenkkan EJ. 1972. On the nasal tract complex of *Pontoporia blainvillei* Gervais and d'Orbigny 1844 (Cetacea, Platanistidae). *Investigations on Cetacea* **4:** 83–90.

Schenkkan EJ. 1973. On the comparative anatomy and function of the nasal tract in odontocetes (Mammalia, Cetacea). *Bijdragen tot de Dierkunde* **43:** 127–159.

Sereno PC. 2007. Logical basis for morphological characters in phylogenetics. *Cladistics* **23:** 565–587.

Thewissen JGM, **Cohn MJ**, **Stevens LS**, **Bajpai S**, **Heyning J**, **Horton WE. 2006.** Developmental basis for hind-limb loss in dolphins and origin of the cetacean bodyplan. *Proceedings of the National Academy of Sciences USA* **103:** 8414.

Thewissen JGM, **Cooper LN**, **George JC**, **Bajpai S**. **2009.** From land to water: the origin of whales, dolphins, and porpoises. *Evolution: Education and Outreach* **2:** 272–288.

Thewissen JGM, **Heyning JE. 2007.** Embryogenesis and development in *Stenella attenuata* and other cetaceans. In: Miller DL, ed. *Reproductive biology and phylogeny of*

Cetacea: whales, porpoises and dolphins. Enfield: Science Publishers, 305–327.

Thewissen JGM, **Williams EM. 2002.** The early radiations of Cetacea (Mammalia): evolutionary pattern and developmental correlations. *Annual Review of Ecology and Systematics* **33:** 73–90.

Thornton SW, **Mclellan WA**, **Rommel SA**, **Dillaman RM**, **Nowacek DP**, **Koopman HN**, **Pabst DA. 2015.** Morphology of the nasal apparatus in pygmy (*Kogia breviceps*) and dwarf (*K. sima*) sperm whales. *The Anatomical Record* **298:** 1301–1326.

Wei C, **Au WWL**, **Ketten DR**, **Song Z**, **Zhang Y. 2017.** Biosonar signal propagation in the harbor porpoise's (*Phocoena phocoena*) head: the role of various structures in the formation of the vertical beam. *The Journal of the Acoustical Society of America* **141:** 4179.

Wei C, **Zhang Y**, **Au WW. 2014.** Simulation of ultrasound beam formation of baiji (*Lipotes vexillifer*) with a finite element model. *The Journal of the Acoustical Society of America* **136:** 423–429.

West-Eberhard MJ. 2003. *Developmental plasticity and evolution*. New York: Oxford University Press.